IEEE Access
Multidisciplinary | Rapid Review | Open Access Journal

Date of publication xxxx 00, 0000, date of current version xxxx 00, 0000.

*Digital Object Identifier 10.1109/ACCESS.2025XXXXX*

# From Pixels to Prognosis: Deep Learning Methods in Abdominal Aortic Aneurysm Imaging

**AIMILIA NTETSKA[1], PANAGIOTIS N. SMYRLIS[1], FOTEINI DIMARAKI[1], KATERINA D. TZIMOURTA[1], MARKOS G. TSIPOURAS[1] and PANTELIS ANGELIDIS[1]**

[1]Department of Electrical and Computer Engineering, University of Western Macedonia, 50150 Kozani, Greece (e-mail: mtsipouras@uowm.gr)

Corresponding author: Markos G. Tsipouras (e-mail: mtsipouras@uowm.gr).

Aimilia Ntetska and Panagiotis N. Smyrlis contributed equally to this work.

This research has been financed by the Operational Program Greece 2.0, under the call Flagship actions in interdisciplinary scientific fields with a special focus on the productive fabric – National Recovery and Resilience Fund. (SAFE-AORTA project, code: TAEDR-0535983)
This article has supplementary material provided by the authors and color versions of one or more figures available at https://doi.org/XX.XXXX/XXXXXXXXXXXX

**ABSTRACT** Abdominal Aortic Aneurysm (AAA) is a vascular disease characterized by abnormal dilation of the lower segment of the aorta (abdominal aorta), resulting from structural weakening and deformation of the aortic wall. Advanced imaging techniques, such as Computed Tomography (CT) and Magnetic Resonance Imaging (MRI), provide rich representations of a subject's clinical condition, while recent studies have explored automated decision support using Deep Learning (DL). This review aims to summarize the current research efforts applying DL to AAA volumetric imaging, focusing on core tasks such as classification, detection, segmentation, and quantification. The methodology entails a systematic analysis of the relevant literature to focus on the types of DL architectures in use and preprocessing techniques commonly employed in decision support pipeline. In total, 67studies are reviewed. The reviewed studies report a wide variety of DL architectures, with segmentation tasks achieving high performance often exceeding 90% in evaluation metrics such as the Dice Similarity Coefficient. This review provides a comprehensive overview of present-day capabilities and limitations as the base for further work on DL-based AAA decision support systems.

**INDEX TERMS** Aneurysm, Abdominal Aortic Aneurysm, Deep Learning, Deep Neural Networks, Computed Tomography, Magnetic resonance imaging, Medical imaging, Image processing, Convolutional Neural Networks, Artificial Intelligence in Healthcare

## I. INTRODUCTION

ABDOMINAL Aortic Aneurysm (AAA) is a progressive vascular condition, typically characterized by a localized dilation of the abdominal aorta, which is defined by an increase in diameter of 50 % compared to the healthy aorta. This condition is usually asymptomatic and is often not diagnosed until rupture, which is associated with a high mortality rate, with estimates ranging from 50% to 90%. [1], [2] AAA has a high mortality rate and an increasing prevalence along aging. Smoking, male sex, and a positive family history are the main risk factors for AAA [3]. Pathophysiologically, an AAA results from structural degeneration of the aortic wall, including thinning of the adventitia and media, extracellular matrix breakdown, and apoptosis of smooth muscle cells.

Early diagnosis and accurate assessment of AAA progression are crucial, since rupture risk increases with aneurysm diameter and causes a potentially fatal intraabdominal hemorrhage. Patients with AAA ruptures record a 65–85% death rate. AAAs can rupture at any size; however, the risk of rupture increases with diameter [4]. The size and growth rate of aneurysms affect the management techniques, and open surgery or endovascular aneurysm repair are two possible treatments [5].

Imaging plays a pivotal role in the diagnosis, treatment planning and follow-up management of AAA. Ultrasound is the most recommended tool as the first screening method, given its excellent sensitivity and specificity in combination with overall safety and cost-effectiveness. Computed Tomography Angiography (CTA)[6] is considered the gold standard for preoperative planning and surveillance, providing detailed information on the morphology of the aneurysm and the surrounding structures. CTA offers superior spatial resolution, making it possible to precisely measure the size of the aneurysm and visualize the aortic architecture in great detail [7]. Magnetic Resonance Imaging (MRI), though less commonly utilized, shows promise for future use in AAA

evaluation and rupture risk prediction [8].

In recent years, the availability of advanced imaging data has motivated the development of automated analysis tools, with Deep Learning (DL) emerging as a key technology. DL techniques, Convolutional Neural Networks (CNNs), in particular, have demonstrated great promise in automating AAA-related tasks such as calcifications, thrombus, and aneurysmal lumen segmentation [9], [10], [11]. Additionally, DL models have shown good accuracy in a variety of clinical situations for risk prediction and disease progression forecasting [12], [13], [14].

Despite these promising advances, significant challenges remain. The lack of large, annotated datasets limits the training and generalization of DL models. Most publicly available datasets are institution-specific and lack diversity, which hinders cross-center reproducibility. Moreover, technical barriers, such as variations in imaging protocols, scanner configurations further complicate model deployment. In addition, the "black-box" nature of DL models further complicates clinical adoption. Regulatory approval and interpretability remain pressing concerns for real-world deployment.

As a result, a thorough evaluation of the state of DL applications in AAA imaging continues to be necessary. Even though a number of studies present promising results, a thorough synthesis is required to comprehend the approaches used, spot performance patterns, and point out any gaps that should be filled by further study.

The purpose of this systematic review is to summarize recent findings on the use of volumetric imaging modalities Computed Tomography (CT) [15], Computed Tomography Angiography[16] and the broader domain of Contrast Enhanced Computer Tomography (CECT) techniques, so as the Non-Constrast CT (NCCT), Magnetic Reasonance Imaging[17], and Positron Emission Tomography (PET/CT) [18]) for the analysis of AAA based on DL. In order to identify trends, limits, and future research paths toward clinically deployable decision support systems, we provide an overview of the DL architectures employed, tasks (segmentation, detection, and classification), and preprocessing pipelines.

## II. RESEARCH METHODOLOGY

This work is carried out according to the Preferred Reporting Items for Systematic Review and Meta-Analysis (PRISMA) [19] Guidelines in order to acquire relevant research. The authors also performed a comprehensive screening procedure, and further quantitatively evaluate the risk of bias of each included study and to determine the eligibility of the articles and their robustness to construct a reliable solution to the problem of interest: the Abdominal Aortic Aneurysm (AAA) screening. The researchers' observations and considerations were settled by a thorough discussion. Finally, a detailed Risk of Bias assessment was performed to quantitatively measure a number of known researchers'concerns about the' robustness and applicability of DL models, following the outline of QUADAS-II [20] system to evaluate all distinct pipelines on the performance of their DL modules.

### A. DATA SOURCES

In February 2025, a thorough search was conducted to obtain all pertinent papers published in the last decade from the literature. The search was performed in the databases:

1) Science Direct
2) IEEEXplore
3) Scopus
4) PubMed

The query ("deep learning" OR "cnn" OR convolutional OR transformer) AND (mri OR CT OR cta) AND (abdominal aortic aneurysm) was applied across all databases for the keyword query defined, due to the limitation of 8 Boolean operators found, for the same query to be defined in every database of interest. This query includes keywords for the search terms of interest, while several extra meaningful word variations were applied where possible, forming the extended string: ("deep learning" OR "cnn" OR "convolutional" OR "transformer") AND ("mri" OR "magnetic resonance imaging" OR "ct" OR "Computed tomography" OR "cta" OR "Computed tomography angiography") AND ("abdominal" AND ("aortic" OR "aorta") AND "aneurysm").

The objective of this search was to identify studies published in the past decade that focus on the application of DL techniques for the detection or segmentation of abdominal aortic aneurysms in biomedical imaging and early diagnosis. All retrieved papers were screened with the use of Rayyan software [21]. Rayyan is an online software specifically designed to support the conduct of systematic reviews and other types of literature reviews. It features a user-friendly interface that enables reviewers to import and manage articles, collaborate seamlessly with team members, and efficiently screen and categorize studies according to predefined inclusion and exclusion criteria.

A total of 1,921 papers were retrieved. Duplicate entries were identified and removed, and studies that did not meet the inclusion criteria were excluded from further consideration. After the first filtering stage, 1,001 unique articles remained. The next step involved screening for titles and abstracts to assess how relevant each study was to the research question. This was done based on some predefined eligibility criteria to find out which studies used DL methods to detect or segment AAA from medical images. As a result, 97 articles were selected for full-text review to determine inclusion in the final analysis. Fig. 1 shows the PRISMA flow diagram.

### B. INCLUSION CRITERIA

This review focuses on deep learning-based approaches applied in biomedical imaging for the detection or segmentation of AAA or the aneurysmal region. The following major inclusion criteria were used to choose the studies of interest:

1) Use of real (non-synthetic) medical images acquired from CT, CTA, MRI, or multimodal imaging including at least one of these modalities.
2) Application of DL algorithms and image processing methods for detection or segmentation tasks.

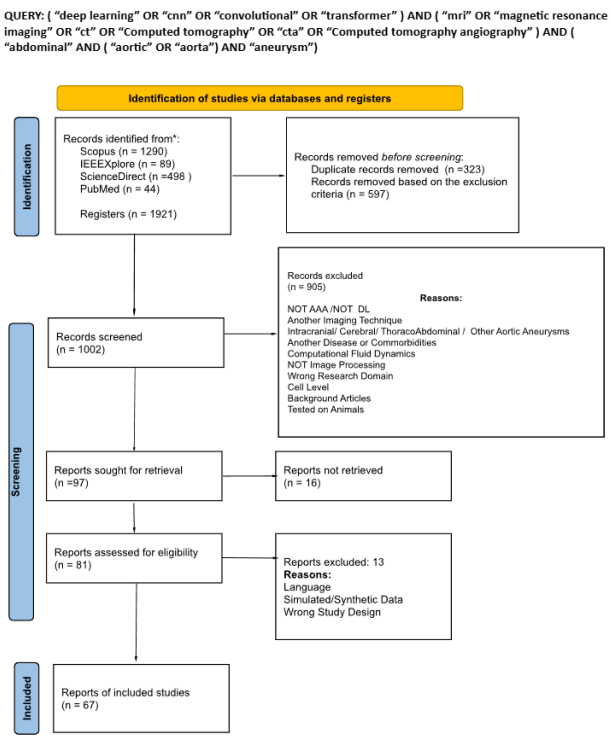


**FIGURE 1. PRISMA Flowchart presenting search query, search strategy followed, database selection, screening process, and exclusion criteria applied to this review.**

3) Inclusion of patients who have been diagnosed with AAA, as confirmed by radiological imaging data.

This review consists of studies using various DL techniques (e.g., Convolutional Neural Networks, Transformers, Yolov8) applied in real imaging data. The purpose of this review is to provide an overview of recent advances, current challenges, and potential clinical applications of deep learning-based approaches for AAA detection and segmentation in biomedical imaging, with particular emphasis on the use of real-world medical data and the importance of accurate and automated analysis for improved diagnostic support.

### C. EXCLUSION CRITERIA

A number of publications were excluded from this review according to the following criteria:

1) Review articles (these studies have been used for comparison purposes)
2) Book chapters and Encyclopedias
3) Meta-Analysis articles
4) Conference info
5) Non-English Articles
6) Dataset Description Papers
7) Research on animals or cell level
8) NOT Abdominal Aortic Aneurysm
9) Another type of aneurysm or cardiovascular disease
10) Focuses on another imaging technique (PET, Ultrasound)
11) NOT Image Processing
12) No DL techniques applied
13) Focuses on CFD technology
14) No model training
15) Synthetic data
16) Not reporting results

### D. DATA SYNTHESIS

A total of 67 studies met the inclusion criteria and were included in the final review. The relevant data extracted from these studies were systematically analyzed to assess the methodologies, performance metrics, and clinical applicability.

The eligibility criteria are implemented in the last phase. To determine eligibility, more than two distinguished independent researchers skimmed the publications. At first, the researchers read the abstract and title of the publication, then, if necessary, particular sections (such as the Methodology and Discussion) to elucidate the goal and methodology of the work. Each researcher then presented the primary features of the experimental publications on a sheet of data extraction.

A detailed data extraction spreadsheet was created to facilitate easy awareness of the variety of research on deep learning-based techniques for the diagnosis and segmentation of AAAs from medical images. The sheet was used to methodically record and examine important aspects of each study that was included.

In addition to these basic aspects, the spreadsheet further includes qualitative remarks on the clinical relevance of each study, specific goals (segmentation vs. classification), and network architecture or preprocessing pipeline innovations, where appropriate. The included articles were also classified according to the imaging modality (CT, CTA, or multimodal) used. To ensure transparency and reproducibility, this review was prospectively registered on the Open Science Framework (OSF) [22]

### E. DEEP LEARNING ANALYSIS

In the following sections, the methods found are examined for the presence of DL models, the data used, and the semantics that are DL-modeled, as well as their post-processing extensions that may provide insight on additional semantics and metrics. In the following sections, the authors extensively discuss the usage, architecture, and performance of the DL models, as well as the situations that the researchers model this way in an AAA decision support system.

Moreover, the authors thoroughly evaluated the data preparation steps involved in the experimental or model development stages, and the automated data preprocessing functions that complement the decision support by transforming the raw data input into the desired model input or enhance the decision making ability. The latter is considered as selected data transforms of the data format, in order to match the desired DL network input, or the data quality, in order to enhance the

model ability to fit the data. Complementary augmentation methods are seen in the literature, which increase the amount of data and enhance the performance and robustness of the model.

In AAA-related decision making support, as in general data-driven systems, the core data analysis task is classification. Within this, some may decide whether a data entity (image, volume, region) constitutes some specific semantic of interest. These systems include a predefined taxonomy of expert-defined classes, where the incoming data have to fit. The Classification task can be considered as the cornerstone of the more sophisticated tasks of Detection and Segmentation, which imply that the data analysis in the respective abstract layer implies the categorization procedure. To the scope of this review, the DL tasks examined are Classification, Detection, Segmentation, Data Generation, and Forecasting, and we discuss the publications of interest, with respect to the DL task that is being employed and the semantics that are being modeled. In terms of data of interest, on which a model fit, the authors focus on Advanced Imaging Techniques, which produce volumetric voxel data, primarily Computed Tomography and its variations, but are not bound to it.

Subsequently, the distinct publication "clusters" are: 1. Classification methods, 2. Object detection methods, 3. Data Generation methods, which contain works that try to create representative examples of a specified modality, 4. ROI segmentation methods, which implies methods that use some detection technique to reduce the region of interest prior to segmenting an image or volume, 5. Volume segmentation techniques for modeling the aneurysmal aorta, 6. Single-class segmentation techniques, which model some specific aneurysm-related semantics and partially segment the phenomenon of interest, 7. Multiclass Volume segmentation techniques, which model more than two AAA-relevant semantics to the aneurysm estimation task. The latter refers to works that are able to distinguish distinct Lumen and Thrombus pixels, while they may additionally model other anatomical structures, too, and they also usually segment the entire data volume.

Regarding the respective results, major representative metrics were also recorded to perform a methods' precision comparison. The authors tried to reside any common likewise notes found in manuscripts, as well as to induct metrics of interest to present a comparative analysis. Specifically, we consider Accuracy, Precision and Recall as the base metrics to a thorough evaluation practice, and argue on the effectiveness of the findings for each study using both the positive and negative results that the DL researchers published, but also any insight on misslcassification conditions. Finally, the Dice Simillarity Coefficient metric (which notably equals the F1-Score in terms of the Classification Task) was inducted for all reports that could support it, including cases that reside a confusion matrix only, or Precision/Recall results.

### F. QUALITY ASSESSMENT STATEMENT

In order to assess quantitative insight on the diagnostic accuracy of any research fingings, the authors further follow an evaluation protocol based on a reasonable number of research concern questions. According to a relevant evaluation questionaire, the authors try to argue on the robustness of the models found in this review and their ability to provide useful solutions as modules to a recent automated diagnosis system for the delineation of AAA in Advanced imaging modalities such as Computed Tomography volumes. In this study, the authors select the QUADAS-II outline to consider some recent quality concerns and quantify the research found in the selected review items.

For this purpose, the authors consider the QUADAS-II distinct concern domains with respect to their relevant demands, and estimate the Risk of Bias and Applicability for each distinct point of interest. For all eight domains/points of interest, an estimate of "Low"/"Unclear"/"High" is made, while the eighth domain/point of interest is an overall decision considering all seven of the previous concerns. In order to finally classify a diagnostic study and measure its quality, the authors use the strict "any high" rule to classify it, attempting to result in useful optimization proposals for the relevant research field: the annotated screening of the Healthy or AAA advanced pathology imagery, and the detailed results are also attached and presented in the Results and Appendix section.

## III. STUDY STATISTICS

The articles in this article were published between 2015 and February 2025, as detailed in Table I. The deliberate focus on the past decade aligns with the objective of this review, which is to present a comprehensive overview of the recent progress in DL methods applied in medical imaging for the diagnosis and segmentation of AAA. Given the rapid advances in artificial intelligence and image analysis techniques, publications prior to 2015 were excluded to ensure the review included only new and state-of-the-art developments. Older studies may not be applicable due to previous methodologies, restricted computational capacities, or the absence of today's neural network architectures.

Through focusing on this 10-year time frame, the review provides a structured synthesis of the most recent, relevant, and influential studies as a reference for clinicians and researchers who are keen on developing the use of DL in AAA diagnosis. The selected publications represent two broad categories: peer-reviewed journal articles and conference proceedings, with a combined total of 67studies. Through this carefully curated collection, the review recognizes recent trends, methodology concerns, and novel opportunities to apply DL to AAA detection and segmentation.

### A. IMAGING TECHNIQUE

To better comprehend the landscape of data sources and imaging modalities, this section provides a quantitative breakdown. Figure 2 indicates that CTA was the most common modality used in 39 studies because of its superior vascu-

**TABLE I. Number of Publications per Year (2015–2025)**

| Year | Number of Publications |
|---|---|
| 2015 | 0 |
| 2016 | 1 |
| 2017 | 1 |
| 2018 | 3 |
| 2019 | 5 |
| 2020 | 4 |
| 2021 | 7 |
| 2022 | 16 |
| 2023 | 13 |
| 2024 | 15 |
| 2025 | 2 |
| **Total** | **67** |

lar detail and critical role in AAA diagnosis and operative planning of AAA. Routine CT was the second most frequent, used in 11 studies, demonstrating its application for structural assessment. In other studies, multimodal imaging methods were employed in other studies, including CTA & CT (n = 2), CTA & Ultrasound (n = 1), and a combination of CTA with PET Scan (PET/CT, n = 1), reflecting efforts to combine functional, soft tissue and vascular data. CECT was used in 4 studies, while NCCT was reported in 1 study, some studies using hybrid protocols such as NCCT & CTA (n = 3) and NCCT & CECT (n = 3) to acquire baseline as well as enhanced anatomical data. In particular, phantom CTA was reported in 1 study. These results demonstrate a staggering dependence on high-resolution, contrast-enhanced structural imaging, and more particularly CTA, in AAA-focused DL studies, with modest but growing research on hybrid and functional modalities.

It is important to note that both NCC and CECT fall under the umbrella of CT imaging. NCCT is CT scanning without contrast agent administration. It is particularly useful in identifying calcifications, intramural hematoma, or when contrast is contraindicated. CECT is intravenous delivery of contrast media, which improves vascular architecture and soft tissue delineation, crucial for the evaluation of aneurysm size, wall integrity, and surrounding anatomy. Together, NCCT and CECT provide complementary information that maximizes diagnostic precision in AAA assessment.

While CTA remains a primary approach in AAA diagnosis and surgical planning, a handful of studies have evaluated MRI. The relatively small representation of MRI-based research in the current literature reflects its higher cost, lower availability, and longer acquisition time compared to CT. Nevertheless, MRI provides multiple other relevant advantages including tissue characterization and wall composition, and may assess intraluminal thrombus (ILT) non-ionizing, along with wall stress, and vessel inflammation. MRI may also be used in studies using computational fluid dynamics (CFD) based studies to characterize patients' hemodynamic patterns and wall shear stress distributions, obtaining biomechanical insights. The possible trajectory of MRI in the AAA assessment—particularly biomechanical modeling, CFD simulations, and risk of rupture—indicates its relevance as an underrepresented representation of AAA imaging in DL classification.

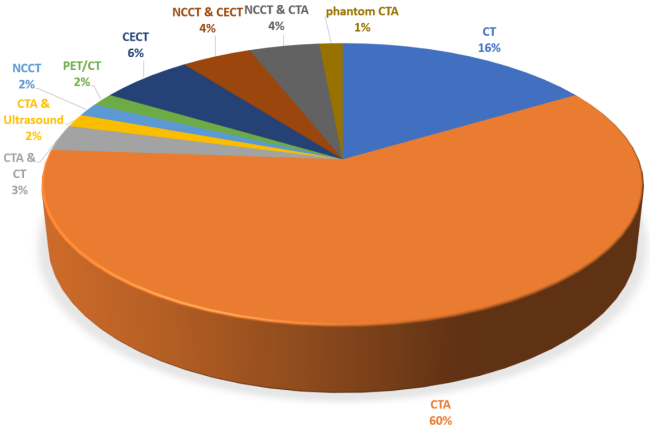


**FIGURE 2. Pie Chart separating imaging techniques used for each paper**

Regarding access to the data sets used, Fig. 3 shows that a significant majority of the data sets used in the reviewed articles are private data sets, originating from collaborating hospitals or health clinics (n = 58). Only a limited number of publications leverages publicly available data (n = 5) and 4 studies use a combination of public and private datasets. This deficit represents the ongoing challenge of data availability and the need for additional open imaging databases to enable reproducibility and greater research effort.

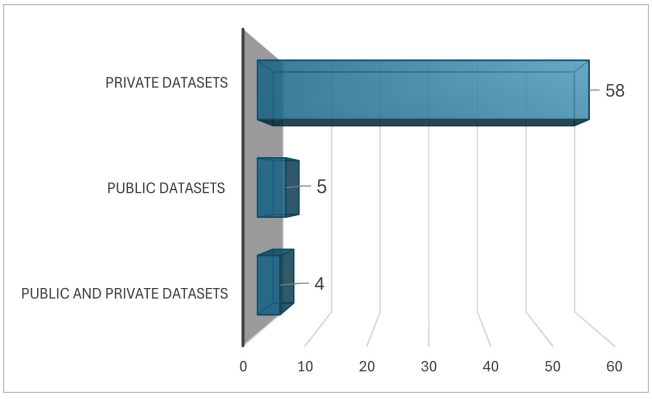


**FIGURE 3. Distribution of private vs. public datasets in reviewed studies**

The public datasets employed by the studies in this review are mentioned in Table II. They, albeit modestly many in number, contribute significantly to promoting transparency,

reproducibility, and benchmarking in the field. The majority of publicly released datasets have abdominal CT or CTA images and vary in anatomical coverage, sample size, and source sites. The release of these data sets has made the segmentation and classification procedures of aortic anatomy and pathology easier. The datasets containing AAA images are the AVT dataset, the Synapse multiorgan dataset and data from University Hospitals Leuven.

The approximate number of images or patient scans ranged significantly across all publications reviewed. To ensure clarity in reporting, the number of patients and the number of CT slices or images are separately analyzed across all included studies. Of the 29 articles in which the patient numbers were explicitly given, the patient numbers ranged from 7 to 950, with an average (mean) value of 186 patients and a median value of 85. In terms of imaging volume, the transverse slice sizes statistics in the included studies are given in Fig. 4. Out of the total 67studies, 40 mentioned a slice size of 512 $\times$ 512 pixels, a standard commonly used in clinical CT for abdominal examination. One study employed a higher resolution of 1024 $\times$ 1024 pixels, implying a desire to maintain more fine anatomical details, and one applied the size of 600 $\times$ 600 pixels, a non-conventional resolution. In addition, four studies used 256 $\times$ 256 pixels, possibly due to computational simplicity or due to limitations in obtaining original images. The remaining studies utilized smaller areas of interest or did not indicate the input image size utilized within their analysis.

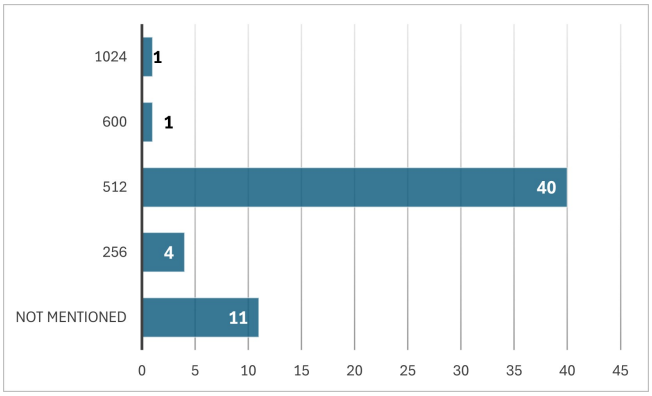


**FIGURE 4.** Size of axial slices employed in studies

### B. PREPROCESING TECHNIQUES

In addition to the selection of appropriate imaging modalities, the reviewed studies used a variety of pre-processing techniques to enhance image quality and model performance. Some of them are utilized for data preparation, while others are embodied in the data processing / DL pipeline as automated functions. Figure 5 presents a quantitative overview of the pre-processing techniques used in the 67 reviewed studies. Most studies have used a combination of techniques; these figure highlights the main techniques employed.

Manual Segmentation is the most common preprocessing technique used by 19 studies, highlighting its central importance in intensity value standardization in imaging datasets. Studies in which CT images were annotated by experts was the next most commonly applied step (8 studies), demonstrating the crucial dependence on expert annotations to supervise the models. Several studies (8) reported proceeding with no preprocessing beyond basic resampling or normalization, demonstrating growing confidence in the ability of modern DL architectures to generalize directly from raw medical imaging data.

Several studies pointed to the utilization of additional preprocessing techniques to improve the robustness of the model. Data augmentation (3 studies) was used to synthetically expand the size and diversity of the data set, minimizing the chances of overfitting. Normalization (5 studies), Region Of Interest (ROI) extraction (4 studies) was also a frequent choice, with the aim of confining the input space to the aneurysmal region and thus enhancing the convergence and precision of the model. Techniques such as filtering and extraction of morphological features were used in a smaller subset of the work to reduce imaging artifacts and emphasize relevant structural information.

More advanced preprocessing pipelines were also described. Windowing techniques, patch extraction with feature reshaping, and intensity normalization through Hounsfield Unit (HU) interpolation were applied in guided methods to enable improved visibility of vascular structures or compensate for acquisition heterogeneity. However, their use was less common than for more routine procedures such as segmentation and normalization.

In short, variability in preprocessing procedures mirrors non-standardization in AAA imaging workflows. This kind of variability would likely contribute, at least partially, to the variance in model performance and generalizability across research studies. Human segmentation and normalization were always ranked among the most critical preprocessing procedures in most of the selected studies, further highlighting their indispensable role in preparing high-quality data for training DL models.

Some of the most prevalent preprocessing steps were not performed individually, but combined with other steps to optimize model training and performance. The following figures show how widespread these combined strategies were in the examined studies.

Figure 6 provides a summary of how manual segmentation was supplemented by other preprocessing operations in all studies. Although 42% of the articles relied exclusively on manual segmentation, others employed techniques such as ROI extraction, intensity rescaling, data augmentation, and filtering. Each of these auxiliary operations is a step towards improving dataset quality and model robustness to variability.

**TABLE II. Public Datasets Employed in This Field**

| Dataset | Number of Articles | Studies | Modality | Data Volume |
|---|---|---|---|---|
| AVT: Publicly available multicenter aortic vessel tree database - Dongyang Hospital | 4 | [23] [24], [25] [26] | CT scans | 50 abdominal CT scans |
| Abdomen data from the Multi-Atlas Labelling Beyond the Cranial Vault challenge - Synapse Multi-organ dataset[a] | 3 | [27] , [28], [29] | CTA | 56 aortas with branches branches |
| University Hospitals Leuven in Belgium | 2 | [30], [31] | CT | 19 CT scans |

[a] The AVT dataset was constructed based on full-body CTA scans, which were taken from the KiTS19 Grand Challenge, the Rider Lung CT dataset, and cases from Dongyang Hospital. All datasets were verified to be publicly accessible as of November 3, 2025.

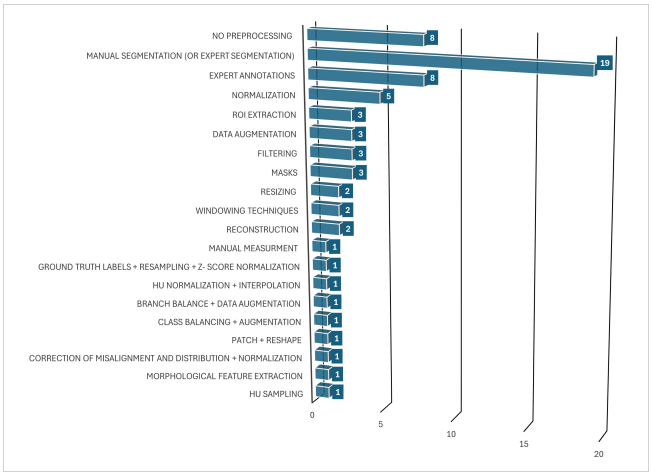


**FIGURE 5. Figure 5. Distribution of preprocessing and data preparation techniques employed across the reviewed studies.**

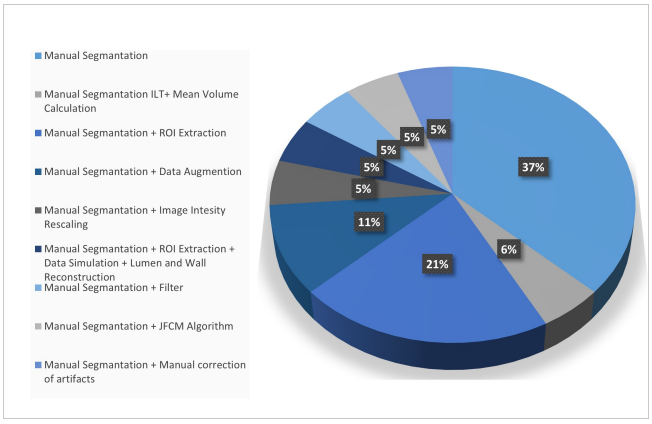


**FIGURE 6. Manual segmentation techniques and their combinations with preprocessing steps.**

Figure 7 illustrates the prevalence of annotation techniques used in all investigated studies. The majority (75%) of the data sets were annotated solely by experts, demonstrating the importance of clinical judgment. A smaller proportion entailed additional Region of Interest (ROI) extraction (12%) or mask creation (13%), reflecting greater but still limited attempts at enhancing annotation accuracy and automation.

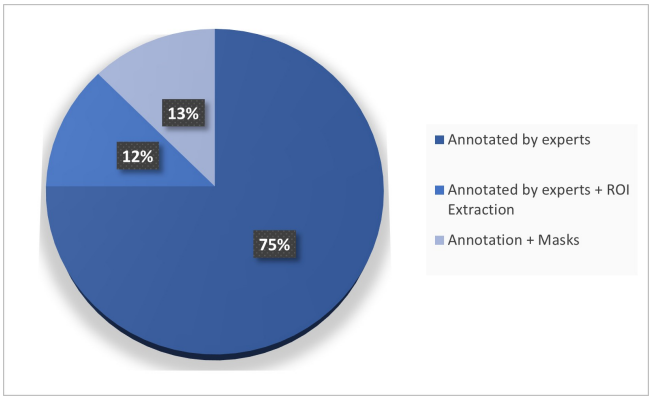


**FIGURE 7. Distribution of annotation approaches across reviewed studies.**

Figure 8 describes the usage of Region of Interest (ROI) extraction across the studies examined. 50% of the studies applied ROI extraction and ground-truth annotation combined with data augmentation, reflecting an integrated approach. The remainder applied plain ROI extraction with augmentation (25%), or sophisticated workflows based on segmentation likelihood maps (25%).

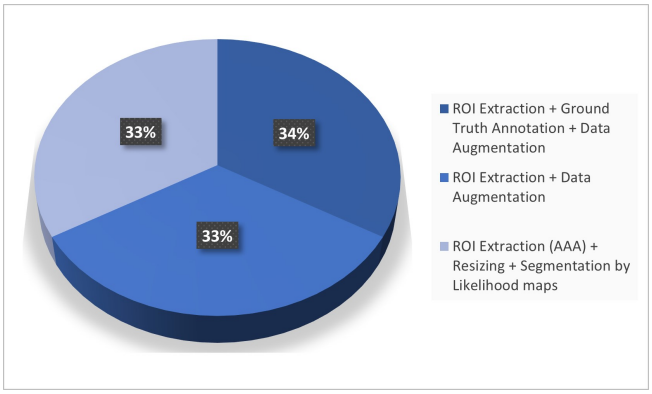


**FIGURE 8. ROI extraction methodologies and complementary preprocessing steps.**

Finally, the breakdown of normalization-associated preprocessing techniques is the same across all fields. The study reflects an even distribution, with each technique—normalization in isolation, normalization paired with resizing, labeling, or augmentation—accounting for 20%.

### C. DEEP LEARNING TECHNIQUES

DL has become the cornerstone technique in the automation of image analysis of AAA. Across the studies considered, various DL models, primarily convolutional neural networks (CNN), were used to perform segmentation, classification, and prediction of disease progression. Current studies also started including transformer-based models and hybrid approaches to improve performance and generalizability.

DL methods used in literature reviews have been utilized for every stage of disease in AAA management. Most studies focused on preoperative imaging, follow-up after surgery, or both simultaneously. Having a good understanding of where these focus are aimed is essential, since this will show whether models are built for early detection, surgical planning, follow-up, or combined disease monitoring. Table III provides an overview of the number of works per disease stage simulated through DL methods. As seen, eight studies have been focusing on modeling postoperative circumstances, such as to estimate the disease progress, or to detect endoleak complications, while the vast majority (49 studies) are strongly interested in preoperative treatment procedures such as early and accurate diagnosis or surgical planning. Finally, a number of studies (8 studies) use prior and post surgical data in their studies, aiming to generalized AAA treatment decision support.

**TABLE III. Disease stages modelled using DL**

| Disease stage | Works |
|---|---|
| Preoperative | 49 |
| Postoperative | 8 |
| Both | 10 |

In addition to disease staging, deep models have been specifically designed to target certain anatomical and pathological features of AAA. The most common semantic targets are the aneurysmal lumen, intraluminal thrombus (ILT), and vascular calcifications. Segmentation and detection of the structures are critical for accurate disease assessment, risk stratification, and therapeutic planning. The semantics defined for each model relies on the researchers' consideration to optimally model the task of interest (e.g. aneurysm detection/segmentation), so respective variations on imaging annotations can be observed. For example, different considerations to the aortic wall modeling can be found, modeling it separately or not, together with the aorta or thrombus classes (as aneurysm).

In terms of modeling different aneurysmal semantics, 5 works were found to distinguish calcifications along the different aorta and thrombus semantics. In one of them [32], the aorta wall is distinctly considered from thrombus, while the rest consider it as part of some other semantic. Within the normal aorta concept, 25 works were found to explicitly model Lumen (usually refers to the aorta without wall), while complemented by an Intraluminal Thrombus class (with or without aorta wall). A separate Intraluminal Thrombus class was named in 25 works (with or without aorta wall). 2 works were recorded to model a separate healthy wall class among lumen and thrombus. Finally, 17 works were observed to perform aorta segmentation tailored to the diseased cases, including the aneurysm to aorta annotation. According to the researchers' considerations, other AAA-related semantics that coexist near the diseased region were also seen in literature. They usually refer to other organ segments or anatomical considerations, like aorta specific regions.

Table IV summarizes the anatomical and pathological features ("semantics") most commonly modeled using DL techniques in the literature. The lumen and intraluminal thrombus (ILT) have each been addressed in 25 studies, highlighting their significance in vascular imaging and disease assessment, particularly in the context of aneurysms. The aorta, specifically in cases with aneurysmal dilation, has been modeled in 17 studies, reflecting growing interest in DL-based aneurysm characterization. Calcifications have been simulated in 5 studies, while the aortic wall has been addressed to relatively fewer studies, only showing in 2 studies.

**TABLE IV. Semantics modelled using DL**

| Semantics | Works |
|---|---|
| Lumen | 25 |
| Aortic Wall | 2 |
| Intraluminal Thrombus | 25 |
| Calcifications | 5 |
| Aorta (with aneurysm) | 17 |

As seen in the literature, the whole range of DL tasks can be employed to tackle aneurysm decision support. Classification works usually consider the automated image labeling problem for the presence of aneurysm in an image, and the preferred taxonomy is binary (aneurysm / not aneurysm), as observed in 9 relevant studies. In terms of the detection task, two works were observed to focus on identifying a region of interest that can be classified as aneurysmal[33], [34], versus the background pixels, while some researchers focused on annotating postsurgical endoleak complications[35]. Likewise, segmentation methods for specific Regions of Interest were seen in 10 recorded studies, which often employ a detection stage to discover a smaller region containing the semantics of interest, followed by a segmentor to pixel-wise assign the classes of interest.

Far more studies (40 works) were observed to perform segmentation on the entire landscape, by sophisticated Deep Learing architectures tailored to the specific requirements

of AAA segmentation. In addition, a study was found to perform predictive analysis to predict complications due to AAA growth [36]. Finally, five works were seen to facilitate data generation, trying to produce rarely found data types and morphologies using more commonly found data.

**TABLE V. DL tasks involved**

| Task | Works |
|---|---|
| Classification | 8 |
| Detection | 3 |
| ROI Segmentation | 10 |
| Segmentation | 40 |
| Forecasting | 1 |
| Data generation | 5 |

In terms of the major operators of the DL architectures, this study discusses network designs that containing convolutional and/or attentional blocks and the Transformer concept. Attentional modules were found to be thoroughly discussed in 8 works, while most of the works over the past decade still strongly rely on convolutional-only modules (59 works). Regarding the major architectures found,

**TABLE VI. DL network modules**

| Modules | Works |
|---|---|
| Convolutional | 59 |
| Attentional | 8 |

### D. PERFORMANCE

In terms of performance reporting and practical implementation considerations, two important dimensions emerged during the synthesis of the included works: quantification and computational cost. Only 18 of studies employed explicit measures of quantification—i.e., aneurysm size, volume, or thrombus burden—within their processing pipeline. This indicates that while segmentation and classification are thoroughly investigated, quantitative analysis to aid clinical decision support is weakly developed. Furthermore, 48 studies reported no computational costs, such as memory requirement, processing time, or hardware configuration. The lack of transparency in the computational resource demand is a hurdle to reproducibility and limits realistic model scalability and deployability estimation in clinical settings.

Moreover, the computational complexity of any data-processing solution is bound to the input size and dimensionality, which leverages the computational costs with respect to the desired computations' individual cost, while in modern medical decision support, the high-resolution data processing is recently questionable. As of the input size observed in this study, most systems (41 works) process 512 sized images (or 512 sided volumes), while only 2 were found to larger sizes (600 and 1024), and 4 studies employed 256 sided input. Empirically, we could estimate that the cost efficiency of likewise methods can always be tuned by reducing the input size, for example, when employing ROI Segmentation instead of whole volume segmentation, but this is also a function of any complementary computations (such as the detection of Region of Interest), so the exact impact on computational cost is subject to the system design architecture and the specific summary of all methods involved.

## IV. RESULTS

This section summarizes key findings from the studies included in this review, focusing on DL applications for the diagnosis and segmentation of AAA. In the current section, an overview of the imaging modalities used, the preprocessing techniques applied, and the DL architectures implemented is presented. Methodological trends, performance metrics, and clinical relevance are also highlighted to assess current capabilities and limitations, and regarding an overall quantified insight of classification precision for the procedures during the last decade, the authors consider the DSC metric as resided by authors, and additionally calculate the DSC whenever considered feasible.

### A. PREPROCESSING AND DATA PREPARATION TECHNIQUES

Data preprocessing and preparation are essential to ensure data consistency, establish model robustness, and increase learning efficiency when using DL in AAA diagnosis and segmentation. One of the suggestions of the reviewer was to create a single taxonomy of preprocessing methods that were reported in the included studies. The details of this are summarized in eight categories: (1) annotation, (2) intensity normalization/windowing, (3) resampling, (4) ROI cropping, (5) filtering/denoising, (6) data augmentation, (7) reconstruction/alignment, and (8) label synthesis.

#### 1) Annotation

Manual segmentation was the most frequently used approach, appearing in 19 studies. This approach involved expert radiologists delineating critical structures such as the aneurysmal lumen, intraluminal thrombus (ILT), and calcifications, which were then used as ground truth for supervised model training. Of these, seven studies implemented manual segmentation as a standalone step to delineate key anatomical regions including the lumen, wall, and thrombus [36], [26], [37], [38], [35], [39]. Four studies combined manual segmentation with extraction of the region of interest (ROI), allowing models to focus on the relevant vascular areas while reducing the computational load [40], [41], [42], [43].

Furthermore, two studies paired segmentation with data augmentation techniques to expand dataset diversity and reduce the risk of overfitting. In one study [44], synthetic data were generated using proprietary algorithms based on surgeon-validated annotations. Augmentation was applied dynamically during model training, with random checks to

ensure annotation accuracy. In another work by Burrows et al. [27], geometric transformations and nonlinear warping were used to increase the dataset tenfold, with 3D space augmentation incorporating random rotations (0°–15°), translations, and scaling (0.7–1.3).

More complex pre-processing workflows were also reported. For instance, Chung's team [45] combined manual segmentation, ROI extraction, simulated data, and lumen-wall reconstruction to develop a high-fidelity training dataset. Other studies applied segmentation with additional refinement steps, including noise-reducing filters [46], the Joint Fuzzy Clustering and Morphological (JFCM) algorithm for boundary enhancement [47], and manual artifact correction [31]. One study combined ILT segmentation with mean volume calculation to allow quantitative assessment of aneurysm burden [48], while another included intensity rescaling to normalize voxel values across patients [37]. Overall, these diverse approaches underscore the centrality of manual segmentation in AAA image analysis workflows.

In addition, nine studies adopted expert-driven image annotation (some semi-automated), reflecting continued reliance on domain expertise for high-quality ground-truth labeling. In several cases, experienced professionals manually delineated ground truth masks [32], [49]. Other studies used these expert annotations to generate pixel-level masks or to extract ROIs [50], [51]. However, the manual nature of these efforts introduces variability and highlights the need for standardized annotation protocols. Finally, manual measurements were reported in one study for validation and feature extraction purposes [52], while additional preprocessing strategies involved handcrafted feature extraction (e.g., short neck, conical or angulated neck, ILT presence, calcifications, and iliac artery features) [53].

#### 2) Intensity normalization / windowing

Building upon the segmentation-based preprocessing, several studies emphasized intensity normalization and windowing to address scanner variability and contrast inconsistencies. Normalization of intensity values was applied in five studies to reduce variation in scanner parameters and tissue contrast. Lyu et al. [54] normalized voxel intensities to the range $[-1, 1]$, while Roby et al. [55] scaled voxel values and resized images from $512\times512$ to $256\times256$ pixels. Wang et al. [56] combined normalization with a labeling step. Mavridis et al. [23] used intensity clipping in the range $[-275, 1900]$ followed by normalization to $[0, 1]$, along with data augmentation (e.g., flipping, rotation, and intensity shifting) and voxel resampling to [1.0, 1.0, 1.5]. HU-based scaling was also reported to standardize CT intensities [57].

Complementary to normalization, window-based preprocessing was reported in two studies. One used window splitting, labeling, and augmentation to improve model learning in localized anatomical regions [58], while another applied a HU window range of 200–500 to enhance vascular contrast, combined with normalization, resizing, and enhancement to improve model robustness [24]. Similarly, Zhang et al. [59] applied interpolation, HU cut-offs, mean variance normalization, and z-score scaling to ensure intensity consistency, while HU-based sampling was used in other studies to capture representative contrast distributions [60].

#### 3) Resampling

Spatial resampling was employed to standardize voxel dimensions and align anatomical structures. One study used resampling and z-score normalization to homogenize voxel intensity distributions [61], while others used B-spline interpolation to correct misalignments and improve geometric consistency across scans [62]. These resampling approaches supported more uniform data representation, facilitating downstream model training and evaluation.

#### 4) ROI Extraction

To further enhance localization and reduce computational demands, ROI extraction was performed in three studies, focusing on the aneurysmal segment. Two of these incorporated data augmentation. Kongrat et al. [63] extracted fixed-size ROI feature maps, applied 3D Slicer for expert annotation, and used augmentation methods such as flipping and grayscale variation, followed by downsampling to $128\times128\times128$ voxels. Li et al. [64] manually placed circular ROIs in three aortic locations and assessed image quality using SNR and CNR metrics. Another study resized cropped ROIs to $256\times256$ pixels for 2D CNN input, reconstructing probability maps as 3D likelihood maps [43].

Similarly, mask-based preprocessing was reported in four studies. Two combined masks with ROI extraction to isolate aneurysmal zones [65], [66]. Salvi et al. [67] used binary masks with downsampling and B-spline interpolation to match CT resolution, while another study applied the same interpolation to align anatomical structures across modalities [68].

Furthermore, two additional studies focused on resizing. In one, DICOM CTA scans were converted to PNG format and resized to $512\times512$ pixels, with thrombus ground truth labeled in the axial plane by radiologists [69]. Another combined resizing with patch extraction, class-wise division, and denoising filters to normalize input size, improve feature localization, and reduce noise for enhanced model performance [70]. Hong et al. [33] further transformed 4-class image patches into feature vectors for model input.

#### 5) Filtering and denoising

Noise suppression also formed an important preprocessing component across several studies. Three works applied filtering to reduce artifacts and enhance image clarity. A denoising filter was applied before segmentation in one case [30], while others used median filters [71] or Gaussian/median filters for artifact suppression [72].

#### 6) Data augmentation

Beyond filtering, several (three) studies emphasized data augmentation as a strategy to mitigate limited data availability

and improve model generalization. López-Linares et al. [73] used intensity-based transformations such as flipping, rotation, and mirroring. In another study [74], ground truth annotations of aneurysm volume and diameter were combined with augmentation strategies. López-Linares' separate work [75] generated synthetic data from 3D B-spline deformation fields and produced six training datasets by varying the ratio of real and synthetic scans, with semi-automatic ground truths manually refined. Another study addressed anatomical asymmetry and class imbalance through branch balancing combined with augmentation [25].

#### 7) Reconstruction and alignment

Reconstruction-based preprocessing was used to enhance anatomical accuracy and spatial fidelity. Epifanov et al. [76] combined reconstruction algorithms with anatomical masks to improve post-processing precision, whereas another study integrated High-Intensity Reconstruction (HIR) algorithms to enhance the visibility of fine arterial structures and suppress noise [77]. These reconstruction strategies helped achieve higher-quality input data for model development.

#### 8) Label synthesis

Finally, a subset of eight studies adopted minimal preprocessing pipelines, performing only basic formatting operations such as image conversion or resizing [78], [79], [29], [80], [81], [82], [83], [84]. This streamlined approach underscores the variability in preprocessing complexity across AAA imaging studies and highlights that, despite the availability of advanced methods, some workflows continue to rely on relatively simple data preparation steps. A few studies performed minimal preprocessing or adopted synthetic label generation strategies to compensate for the scarcity of annotated data, underscoring the need for standardized labeling frameworks in AAA imaging.

To ensure comparability across heterogeneous studies, we consolidated all preprocessing-related operations into a unified taxonomy including annotation, normalization/windowing, resampling, ROI cropping, filtering/denoising, augmentation, reconstruction/alignment, and label synthesis. Figure 9 summarizes the distribution of these techniques across different DL tasks, highlighting that segmentation studies consistently relied on annotation and ROI-based cropping, while augmentation and normalization were less frequently applied.

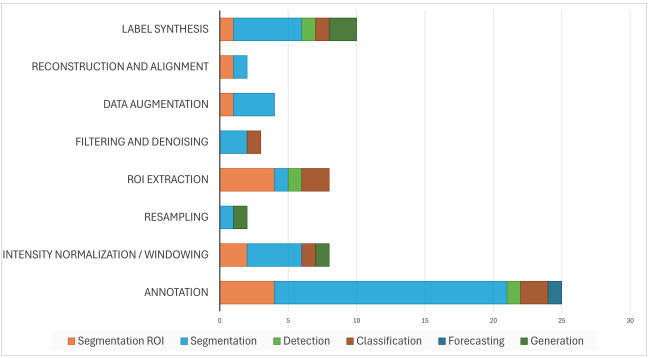


**FIGURE 9. Distribution of preprocessing techniques across DL tasks in AAA imaging studies (n = 68). Stacked bars represent the proportion of studies applying each technique by task type.**

### B. CLASSIFICATION

Within the queried applications, 8 DL classification works have been located since 2019, which architecture was entirely built using convolutional blocks only. A detailed record of the authors' observations on these methods is found in Table VII. Most of them are designed to process visual images with 512 pixel sides, which are inducted from the collected reflections of the computed tomography scanner, transferred to the RGB field, as an expert physician can visually observe [40], [56], [49], [70], [80]. One study was found to include prior and postoperative data[80], while all works focus on the evolution of the disease before surgery and repair. Most methods are trained on CTA data [40], [49], [70], [80], [59], [72], which is considered a "Gold Standard" for AAA screening, while one work declares the likewise CECT technique [85], which is an "umbrella" term of CTA. Moreover, one work [70] declares the CT technique together with CTA, while one model [56] is built on NCCT data.

Almost all methods [40], [56], [49], [80], [59], [72], [85], are trained in the binary classification question wether this region/image is aneurysmal or not, and rely on classic DL architecture design (ResNet[86], VGG[87], AlexNet[88], DenseNet[89], EfficientNet[90]), using a selected (VGG-16) or test a range of proposed flavors (eg ResNet-50, ResNet-152). In contrast, in [70], the Aorta region is spotted among several anatomical structures using a novel image encoder, and an image processing algorithm tries to delineate the exact morphology of the predicted region and estimate the severity of the disease.

The classification methods found can be distinguished as 2D and 3D methods. The former techniques are capable to operate on a single axial view, while the latter operate on the entire volume, or a 3-dimensional region of interest. Image classification, namely methods that operate in two-dimensional plane, are used in [40], [49], [72], [80], [56], usually operating for a specific, or each separate view slice of 3D Volume to make predictions. Recently, some researchers [56], [72], [80] claim an accuracy greater than 99% and between 91% - 99% for the task of recognizing what image

**TABLE VII. Classification techniques**

| Literature | Modality | Semantics | Dimensions | Method | Highlights |
|---|---|---|---|---|---|
| Zhang et al. [59] 2024 | CTA | AAA Not AAA | 3D | ResNet-200 | ROI Voxel 3D Convolutional Feature Extract with machine learning on preoperative data AUC: 85.2% (DL Model test set), AUC: 92.7% (diagnostic pipeline accuracy) |
| Rajmohan et al. [72] 2024 | CTA | AAA Not AAA | 2D | EfficientNetB7 | Image Classification on preoperative data Accuracy: 92%, Precision: 91%, Recall: 90%, DSC: 90.49% |
| Wang et al. [40] 2023 | CTA | AAA Not AAA | 2D | Transfer Learning ResNet-50 | Image Classification on preoperative & postoperative data. Transfer Learning on ImageNet pretrain. CAM visualization to indicate SAEs. AUC: 81%, Accuracy: 82%, DSC: 87% |
| Tomihama et al. [80] 2023 | CTA | AAA Not AAA | 2D | Transfer Learning VGG-16 | Image Classification on preoperative & postoperative axial data. Transfer Learning on ImageNet pretrain. CAM visualization to indicate aneurysm region. AUC: 99.98%, Accuracy: 99.6%, Sensitivity: 98.7%, Specificity: 99.7%, DSC: 99.8% (calculated on Confusion Matrix) |
| Miao et al. [56] 2022 | NCCT | AAA Not AAA | 2D | Transfer Learning ResNet-50 ResNet-152 DenseNet-121 DenseNet-201 EfficientNet-B0 | Image Classification on preoperative axial data. Transfer Learning on ImageNet pretrain. CAM visualization to indicate aneurysm region. Best model: DenseNet-121, ROC-AUC: 99.7%, Accuracy: 99.6%, Recall: 99.8%, Precision: 97%, DSC: 98.2% |
| Camara et al. [49] 2022 | CTA | AAA Not AAA | 2D | Transfer Learning VGG-16 | Image Classification on preoperative axial data. Transfer Learning on ImageNet pretrain. CAM visualization to indicate aneurysm region. AUC: 99%, Accuracy: 99.1%, Sensitivity: 98.9%, Specificity: 99.3%, DSC: 99.08% (calculated on Confusion Matrix) |
| Golla et al. [85] 2021 | CECT | AAA Not AAA | 3D | AlexNet 3D VGG-16 3D ResNet | 3D Voxel classification on preoperative visual data. Layer-wise relevance propagation to create relevance maps. Best model: 3D ResNet, AUC: 97.1%, Accuracy: 95.3%, DSC: 89.4% |
| Mohammadi et al. [70] 2019 | CT CTA | Abdominal Inside Region, Aorta, Body Borders, Backbones | 2D | Novel Encoder | Novel CNN Encoder design. Hough Circles algorithm to define exact aorta borders and measure its diameter. Diameter is converted to mm and AAA risk is estimated with respect to size as no risk, medium risk or high risk. Aorta Detection Accuracy: 98.62% (classification), 98.33% (Hough Circles), Precision: 97.94%, Sensitivity: 97.93%, DSC: 97.93% (calculated on metrices) |

shows an aneurysmal condition, prior to surgery (preoperative data). Transfer weight learning from the common objects' model (ImageNet[91] pre-train) is employed in most works (4 out of 5) to initialize training. Typically, the findings of the researchers are visually resided using Class Activation Maps (CAM) on a high abstract layer to indicate the presence of an aneurysm. In terms of architectures used, all methods found rely on 'classic' DL classification architectures, while their success indicates that their usage remains sound and not obsolete.

To work for three dimensions, the problem remains to discover whether an entire 3D volume or a 3D region of interest contains an AAA. However, Mohammadi et al.[70] have tried to use DL to distinguish relevant organ regions, proposing a novel CNN to the specific disease recognition task, while using image processing to delineate and measure the abdominal aorta and estimate the severity of the disease. Zhang et al. [59], tried to exploit the ability of DL to extract valuable information from raw data, to assess the higher level representation of a 3D CTA volume, to use as a module in a broader decision support system on disease progression, so a classification model is trained, but it is the intermediate representations that are given to the decision support logic and further fused with other information. In [85], a 3D ResNet was trained to perform classification, and then intermediate layer-wise information is reused to create relevance maps that can visualize the presence indicators of the aneurysm. An experimental comparison was made among other known architectures (AlexNet, VGG-16).

**TABLE VIII. Detection techniques**

| Literature | Modality | Semantics | Dimensions | Method | Highlights |
|---|---|---|---|---|---|
| Koçer et al [34] 2024 | CT | AAA | 2D | YOLO | AAA detection on preoperative CT visual images of transverse axial view using Yolov5. ∼80% peak sensitivity and ∼60% peak precision on validation across epoch training to indicate potential applicability of YOLOv5 on AAA localization using 1024 pixel sided images. |
| Hahn et al [35] 2019 | CTA | AAA | 2D | Transfer Learning RetinaNet | Endoleak Detection: RetinaNet AAA ROI localization with ResNet-50 pretrain. Post-processing to remove outliers: removing isolated predictions if too far from a series of predictions. ResNet-50 binary classification to decide if Endoleak is present. Detection Accuracy: 98.7%, Endoleak AUC, Accuracy: 94%, 89% |
| Hong and Sheikh [33] 2016 | CT | AAA | 2D | Deep Belief Network | AAA region detection followed by Bayesian level set algorithm to delineate (segment) Lumen, Thrombus and Calcifications. Detection error rate of 10 and 20% obtained by different configurations for detecting small and large aneurysms. |

### C. DETECTION

The AAA Detection task, usually means to extract the exact rectangular boundary in which an AAA resides. The relevant methods operate on the entire image and try to eliminate the region of interest to a much smaller space. The relevant publications are summarized in Table VIII. All three works examined rely on convolutional modules only. Recently, a YOLOv5-based study was published [34] that claims the potential of the YOLO architecture for AAA detection for higher resolution images (1024p), which can be further examined in practice for this task.

Earlier approaches [35], [33] have tried to localize the AAA ROI, claiming an accuracy above 90% on test data. In [35] a RetinaNet is trained to determine the disease boundaries. A few postprocessing steps in pipeline include the HU intensity values' clipping within a predefined intensity range and outlier removal for bbox predictions that are considered isolated. Consequently, a ResNet-50 is trained on the ROI pixel to determine if this aneurysm contains an endoleak or not. The authors claim an 98.7% AAA detection accuracy and an 94% AUC for endoleak detection.

Deep Belief Networks are employed in [33], where a Bayesian level set algorithm delineates any entities of interest (Lumen, Thrombus, Calcifications) as post-processing. The DL network performs the ROI localization task, and the authors claim an error rate of 10% for the best network configuration.

### D. SEGMENTATION ON REGION OF INTEREST

These works typically present a cascade of autonomous detection and segmentation operations. The detection method is capable of localizing a smaller region of interest out of the entire image, while the segmentation procedure provides pixel-wise annotation on the specified region. The relevant publications are shown in Table IX. The different approaches with respect to the semantic of interest, model an aorta region (which may contain aneurysm) [29], the distinct Lumen & ILT entities [37], [52], [63], [77], maybe complemented with a class of aorta walls, or the AAA pixel mask (thrombosis and wall, without lumen)[39], [94].

CECT (typically CTA) is the modality preferred in this task, too, because of its ability to better highlight the region of the aorta. However, some promising results have yet been published [93], to indicate the possible usability of NCCT that claims precision equal to that of CTA, using U-Net architectures with attention modules in combination for multiclass segmentation of the abdominal aorta. Such results can be further examined with respect to the scope of research for intravenous contrast-free scanning ability.

The methods presented make extensive use of U-Net structured networks, with convolutional and/or attentional modules to the detection and segmentation stages. All report descent success metrics (commonly DSC evaluated), above 80%, or many of them above 90%. The highest reported DSC was found as a result of the ROI segmentation of 3D U-Net in [63] to delineate Lumen and ILT in the CTA subregions that were manually defined. In [29], a regression method is used for localization, while the U-Net segments the region of interest. Segmentation is performed to delineate the aorta, with respect to the aorta section found, followed by conventional image processing methods to pixel-wise extract the Lumen and ILT pixels and provide morphological measurements.

In [52], [93], [37], [57], a likewise schema is also used to detect and consequently segment Lumen and ILT, using an attention mechanism to the segment stage, while in [32] it is used in the detection phase. The semantics discovered are primarily the Lumen and ILT, while [93], [32] include the Aorta Wall and [32] the Calcification entities in the DL pipeline. An ensemble segmentation approach is also located in [39], in combination with VBNet and majority voting. In post-processing, Centerline extraction, connected component analysis, Skeletonization, and morphological measurements (maximum diameter for aorta/lumen/ILT) are provided. Image filtering was also observed to provide noise-free slices in [57].

ResNet-based procedures are observed in [39], [32] for the segmentation and detection task, respectively. The former employs a sliding-window method and subsequently

**TABLE IX. Segmentation on Region of Interest**

| Literature | Modality | Semantics | Detect Method | Segment Method | Highlights |
|---|---|---|---|---|---|
| Ma et al. [92] 2024 | NCCT | Aorta | None | Attention U-Net | 2D Attention U-Net trained on pseudo-labels of preoperative data, derived as regularized original annotations using ellipse fit. Network is trained selecting a 256x256 region of Interest. Attention modules are placed in the decoder. DSC: 85.7%, Sensitivity: 88.7% |
| Postiglione et al. [74] 2024 | CTA | Aorta Ascending aorta Aortic arch, Descending aorta Suprarenal Infrarenal Right iliac Left iliac | NN Regression | Unet | NN Regression for bbox localization and U-Net segmentation on preoperative & postoperative data. Refinement with fuzzy region competition, minimal path algorithm for lumen & thrombus, diameter measurement, volume measurement. DSC: 94% |
| Spinella et al. [52] 2023 | CTA | Lumen ILT | U-net | U-net (Attention) | ROI identification with U-Net. Each single axial view U-Net segmentation. 3D integration using simple averaging. Centerline Extraction, Z-axis connected components analysis, Skeletonization algorithm, Maximum Aorta Diameter calculation. Accuracy: 97%, Sensitivity: 98%, Specificity: 96% Segmentation DSC: 91% (ready-made pretrained segmentor) |
| Abdolmanafi et al. [32] 2023 | CT CTA | Wall lumen ILT Calcifications | Transfer learning Resnet-18-based | Resnet-18-based | Three trained networks for AAA segmentation on preoperative data: 1. ROI identification and segmentation, 2. Lumen extraction and ILT identification. 3. Calcified ROI Classification, 4. Landmark Detection (aorta anatomical segments). Segmentation mean IOU: 97.5% (test set),90% (external test set)/. DSC: 98.73%, 94.73% (calculated on IOU for test and external test set), Classification Accuracy, Sensitivity, Specificity: 81% - 91% |
| Chandrashekar et al. [93] 2023 | NCCT CTA | Wall Lumen ILT | Attention U-net | Attention U-net | 1. Aortic ROI Detection (Unets A & D for NCCT and CTA) 2. Aortic Segmentation on ROI (Unets B,C for lumen/wall segmentation on thoracic/abdominal ROI) and 3. Abdominal aorta segmentation on NCCT. DSC: 95% (CTA, Thoracic), 93.7% (CTA, Abdominal), 93.5% (NCCT, Abdominal) |
| Brutti et al. [37] 2022 | CTA | Lumen ILT | U-net | 3D U-net | AAA segmentation on preoperative data: 1. Aortic centroid identification, 2. ROI cuboid crop, 3. Segmentation, 4. Centerline extraction, 5. Mean maximum total aneurysm diameter calculation, 6. Mean lumen diameter calculation. DSC: 89% |
| Kongrat et al. [63] 2022 | CTA | Lumen ILT | None | 3D U-Net | 3D U-Net, doubled values of the channels before each max pooling to segment preoperative data. Region of interest (128x128x128 voxel) was manually cropped. DSC: 98.68% |
| Adam et al. [77] 2021 | CTA | Lumen ILT | Novel Detect CNN | VNet | AAA segmentation on preoperative and postoperative data: Novel detect CNN to detect ROI bbox and VNet to segment AAA. Segmentation Refinement: fuzzy region competition, centerline extraction: minimal path algorithm, Diameter measurement: max diameter as the maximum of slices. DSC: 84% (healthy), 95% (diseased), and 93% (diseased aortas after endovascular treatment) |
| Dziubich et al. [39] 2020 | CTA | AAA | ResNet-50 | Unet, VBNet ensemble | AAA segmentation on postoperative data. ResNet-50 bbox localization with overlapped sliding window. Ensemble of 3D U-Net and VBNet96 with majority voting to AAA segmentation. DSC: 94% |
| Fantazzini et al. [57] 2020 | CTA | Aorta | U-net | U-Net | 128x128 Bbox localization using U-Net. 3D cuboid and multi-view aggregation by concatenating the 2D probability maps and applying a Gaussian filter along the z-direction DSC: ∼93%, Average surface distance: ∼80% |
| López-Linares et al. [94] 2018 | CTA | ILT (with wall) | DetectNet | modified HED network | ILT detection on postoperative data. Detectnet to localize the Region of Interest. ROI segmentation using modified HED network: novel network architecture that detects edges but preserves the shape and appearance information of the thrombus. DSC: 82%. |

segments the ROI. In post-processing, an identification of the landmarks for the aorta regions follows the segmentation method, scoring 94% DSC in overall. The latter performs Autoencoder segmentation by training separate networks for the Region of interest and the Lumen/Thrombus segmentation, and consequently performs wall classification as calcified or not, scoring 97%-99% BF-score for segmentation and 81%-91% for metrics in calcification recognition.

### *E. VOLUME SEGMENTATION METHODS FOR ENLARGED AORTA*

These techniques, which are summarized in Table X, model AAA detection as aorta deformations and compute all pixels of the aorta, including Intraluminal Thrombus regions. Most of the data used in these studies come from contrast-enhanced computed tomography scans [11], [26], [84], [24], [46], [47], [31], [67], while the focus is on the segment of the aorta organ.

The variants of the U-Net schema for two- or three-dimensional processing are commonly found in most studies [95], [28], [26], [30], [24], [46], [31], [38], [67]. Some researchers propose slice-by-slice segmentation (2 dimen-

**TABLE X. Volume Segmentation methods for Enlarged Aorta**

| Literature | Modality | Semantics | Dimensions | Method | Highlights |
|---|---|---|---|---|---|
| Wan et al. [50] 2024 | CT | Aorta | 2D | Encoder-decoder | 2D Encoder-decoder architecture with attentional modules. Feature extraction by image processing and feature fusion. Segmentation on preoperative and postoperative data. Precision: 97.32% (all data), Sensitivity: 90.01%(preoperative), 86.2%(postoperative), DSC: 93.29%(preoperative) , 91.01% (postoperative) |
| van Praagh et al. [95] 2024 | PET/CT | Ascending aorta Aortic arch Descending aorta Abdominal aorta | 3D | U-Net | 3D U-Net segmentation on preoperative data. Image processing operations for Calcium calculation, Radiomics Feature Extraction, 2D Visualization, Background Measurements. DSC: 88.5% (internal test set), 86.7% (external test set) |
| Chatterjee et al. [28] 2024 | CT | Aorta | 3D | U-Net | Previously published modified 3D U-Net for aorta segmentation on preoperative data. 2D images extracted from 3D prediction to perform ellipse fitting for maximal diameter calculation. Automated calcified atherosclerotic plaque detection. Sensitivity 96% (95% CI 89%, 100%), Specificity: 96% (96%, 97%), AUC: 99% (98%, 99%), DSC: 94% |
| Smyrlis et al. [51] 2024 | CTA | Aorta | 2D | YOLO | YOLOv9 and v8 models trained on CT visual images of preoperative CTA data. Multi-versions' and flavors' model comparison on preliminary test data for precision and resource efficiency. Best model (v9-C) Sensitivity: 100%, Precision: 98.97%, mAP50-95: 76.15% , DSC: 99.48% |
| Mu et al. [26] 2023 | CTA | Vasculature | 3D | Cascade U-Net based | Two 3D U-Nets in cascade. Initial segmentation result by the 1st U-Net (low resolution) guides the 2nd U-Net (full resolution). Frequency-domain channel attention module using the Fourier Transform, together with spatial attention. 3D model visualization. Sensitivity: 95.68% Specificity: 99.97%, DSC: 89.9% |
| Saleem Javeed et al. [30] 2023 | CT | Aorta | 2D | U-Net | U-Net image segmentation trained on preoperative data. Postprocessing using morphological approaches with region growth (Erosion and dilatation to fill holes and remove artifacts) and network finetuning. Sensitivity: 89% Specificity: 97%, DSC: 81% |
| Zhang et al. [84] 2023 | CTA | Aorta | 3D | Encoder-Decoder LSTM | Encoder-Decoder architecture trained on preoperative data. 2D Feature extraction and an LSTM module in encoder and an attention module in decoder. DSC: 91% |
| Benčević et al. [24] 2022 | CTA | Aorta | 2D | U-Net based | Polar transform for annotated elements and centroid extraction. Data augmentation using centroid jitter. Modified 2D U-Net trained on polar data. Sum of predictions converted to normal coordinates and thresholded by confidence of being aorta. Sensitivity: 97.3%, Precision: 91.5%, DSC: 93.2% |
| Dziubich et al. [46] 2021 | CECT | Aorta | 2D | Ensemble based on U-Net, ResNet, and VBNet | Image processing to image denoising and DL training on preoperative data. Whole volume CT segmentations construct a 3d surface, while smoothed with an image and surface filter. Centerline extraction. DSC: 91% |
| Zheng et al. [47] 2021 | CTA | Aorta | 2D | Novel CNN | CNN trained on preoperative data for segmentation and denoising. JFCM algorithm was used to filter features adaptive median filter for denoising, and a novel cnn architecture. Accuracy: 92.86 - 94.9%, Sensitivity: 95.45 - 97.73%, Specificity: 70% |
| Salvi et al. [67] 2021 | CTA | Aorta | 3D | U-Net based | Modified U-Net using LeakyRELU activations trained on preoperative data. Finetuning by retraining on additional data. DSC: 75% (Lumen) |
| Habijan et al. [31] 2020 | CTA | Aorta | 3D | U-Net based | Modified 3D U-Net using deconvolution at decoder, trained on preoperative data. DSC: 91.03% |
| Zheng et al. [38] 2019 | CT phantom CT | Aorta | 3D | U-Net | 3D U-Net trained on preoperative data. Skeleton Graph Construction considering adjacency rules. CT and fluoroscopic skeletons' matching algorithm to infer skeleton deformations. 2D distance error (pixel): 0.12 on patient data, 0.11 and 0.08 on phantom and simulated data. 3D distance error: 2mm on phantom data, 1.13mm on simulated data |

sions). In [46], an ensemble containing ResNet and VBNet is also proposed, while the 3D visual model includes image smoothing, a surface filter, and centerline extraction.

A novel U-Net variant based on the polar coordinate transformation was also seen in [24], while finally the polar-coordinated predictions are thresholded before being transformed back to normal coordinates. In terms of 3D processing, a cascade variant of U-Net is shown in [26], which aims to delineate the whole vascular system. Further architectural innovations are resided using the Fourier transform and tailored attention modules, claiming an about 90% DSC score, while a 3D visualization is embedded. In post-processing following the U-Nets, calcium calculation by image processing [50], [95], ellipse fitting for maximal diameter calculation, radiomics feature extraction, erosion & dilatation, and skeleton extraction.

Another approach is built on the YOLOv9 [51] architecture for image segmentation, while other researchers have tried to synthesize a novel CNN [47] with feature median filtering to model aorta organ annotation on CTA. A novel approach has been further proposed in [84], where an encoder-decoder module is complemented by an LSTM to integrate the third dimension insight.

### *F. SINGLE CLASS SEGMENTATION FOR AAA-RELATED ENTITIES*

Some works, which are shown in Table XI, focus on one specific semantic that is related to the AAA disease, presenting

**TABLE XI. Single-class segmentation approaches on AAA-related semantics**

| Literature | Modality | Semantics | Dimensions | Method | Highlights |
|---|---|---|---|---|---|
| Lyu et al. [81] 2024 | CTA | AAA Wall | 3D | 2d Unet ZoomNet | U-Nets trained for single-view segmentation of preoperative data. A fourth U-Net is trained to perform multi-view integration using all three views. Sensitivity: 92%, DSC: 88% |
| Hwang et al. [69] 2022 | CTA | AAA wall | 2D | Mask-RCNN | Thrombus segmentation on postoperative data visual images using Mask-RCNN. A modified focal loss for classification is employed. DSC: 82.67% |
| Salvi et al. [61] 2022 | CTA | AAA Wall | 3D | U-Net based | U-Net based CNN for thrombus segmentation on postoperative data. Encoding CNN blocks, upsampling decoding and the parametric rectified linear unit (PReLU). Training on 128x128x128 region of interest. DSC: 42% (asymptomatic cases), 32% (symptomatic cases) |
| Siriapisith et al. [81] 2022 | NCCT CECT | AAA region | 3D | Transfer Learning AG-DSV-UNet | Data enhancement embedding coordinate information. DL networks trained for preoperative and postoperative data. Transfer Learning for postoperative data training. Best model (AG-DSV-UNet) DSC: 97.13%(NCCT), 96.74% (CECT) |

novel modeling methods to its precise delineation. In [81], the authors extract AAA as a distinct entity that includes the aorta or other semantics found within the aneurysm boundary. The study also includes data enhancement by combining CT data with the respective coordinate information to increase performance. U-Net-based models in [81], [61] are used for the preoperative and postoperative AAA thrombus 3d segment in CTA volumes, experiments indicating descent performance (DSC: 82.67%, 88%) to handle preoperative examples.

In [69], Mask-RCNN image segmentation presents likewise ability to perform the same task in two dimensions. With the addition of a novel focal loss function for classification, the authors claim an DSC 82%, for AAA wall segmentation for CTA slices / images.

Siriapisith et al. [81] makes use of both NCCT and CECT preoperative data to train various models, fused with coordinate information. The authors claim 97.13% and 96.74%, respectively, by AG-DSV-UNet, and further use transfer learning to model postoperative data, scoring 94.90% and 95.66%, respectively.

### G. MULTICLASS VOLUME SEGMENTATION METHODS FOR INTRALUMINAL THROMBOSIS

Regarding the multiclass segmentation approach, Table XII contains DL methods that are able to annotate more than two semantic classes and segment the entire CT volume to distinguish AAA and the aorta. The semantics of interest are commonly the Lumen and the ILT, but also the Calcifications [78], [76], Stent [27], Spine [71], or other organ structures [79]. The ILT class may also be seen as the thrombus, or some delineation of the entire aorta wall that includes any thrombotic mass [55], [45]. The volume modalities declared are NCCT[65], CECT[27], CT[78], [76] and CTA[55], [79], [23], [96], [97], [41], [44], [53], [45], [42], [71]. In post-processing, various volume measurement methods are employed to complement the decision support. Some of them are the diameter of the aortic neck, the diameter of the aortic region, the angulation of the aortic region [78], the length of the segmentation, the surface, the radius, the torsity [66], and 3D visualization.

Ma et al. [65] presented an autoencoder approach that includes a feature fusion logic, reporting a DSC 88.7% in preoperative CTA data. Jung et al.[41] proposed Mask-RCNN image segmentation followed by a Bi-CLSTM to model three-dimensional volume information, reporting 87.3% DSC. In [27], a Variational Autoencoder is trained for postoperative CECT data using their edge detection transformation, reaching 90.9% DSC for ILT and 93.7% for the semantics of Lumen and Stent. In [40], a DeepLabv3+ architecture is employed with a ResNet-50 pre-train (Transfer Learning) to distinguish ILT and Lumen, reaching a BF score of 98.29% assessed with a train / test setup.

Other approaches, mainly operating on CT and CTA, employ some U-Net schema for segmentation. Recently, Roby et al. [55] reported a DSC of 95.62% and 96.5% for the classification of Lumen and outer wall pixel. Other U-Net variants seen, like the U-Net ensemble [78], Cascade U-Net [97], nnU-Net[96] and U-Net based novel approaches [79], [23], [76], [44], [45], [71] reported a minimum 83.12% DSC success in testing.

### H. DATA GENERATION

The data generation task includes the ability to create synthetic data for modalities that are not commonly found to feed neural network training. Typically, Generic Adversarial Network algorithms are found to perform some image to image translation and provide some approximation of how would it be if a given image was transformed to another target imaging technique. For training, a generator is trained to perform the translation task, while a discriminator is to measure the result success.

In [60], [54] an NCCT to CTA method is employed, while in [62] the target modality is CECT to generate contrast enhanced imagery out of non-contrast CTs. In [29], an intermediate representation based on Ultrasound and CT is produced to tackle the lack of annotated Ultrasound datasets. The CT annotations are encoded and mapped to simulated Ultrasound images. The features inducted by the model are used to model real Ultrasound aorta segmentation. Finally, in [64], a CTA reconstruction method is used to produce synthetic CTA and enhance the low-dose CT predictions, providing more separable data.

**TABLE XII. Multiclass Volume Segmentation methods for Aorta and thrombus**

| Literature | Modality | Semantics | Dimensions | Method | Highlights |
|---|---|---|---|---|---|
| Roby et al. [55] 2025 | CTA | Lumen Outer Wall | 2D | U-Net | 2D U-Net trained on preoperative data and images sized to 256x256. User interactive NURBS-Based tool including segmentation refinement and enhance. 3D model reconstruction using segmentation masks. DSC: 95.62% (Lumen), 96.58% (Outer Wall), 96.1% (mean calculated) |
| Zhang et al. [79] 2025 | CTA | Lumen Left & Right Renal Artery Sup. Mesenteric Artery Aneurysm | 2D | U-Net based | 2D U-Net based architecture on preoperative data. Novel feature fusion and extraction method. Self attention mechanism, Convolution, Attention, upsampling decoding. DSC: 87.6% |
| Mavridis et al. [23] 2024 | CTA | Aorta Aneurysm | 3D | U-Net | 3D U-Net trained on preoperative data. Marching cubes algorithm to generate the reconstructed surface geometries, as a 3D surface model. DSC: 89%, Sensitivity: 90% |
| Kim et al. [78] 2024 | CT | Aorta Thrombus Calcifications | 2D-3D | U-Net ensemble | 2D-3D U-Net ensemble on preoperative data. Landmark extraction for automated measurements on 3D model: aortic neck diameter, aortic aneurysm diameter,right iliac artery diameter, left iliac artery diameter, aortic neck length, common iliac artery tortuosity, aortic neck angulation DSC: 92.8% (Aorta), 78.2% (Thrombus), 70.2% (Calcifications), 80.4% (calculated average) |
| Ginzburg et al. [96] 2024 | CTA | Aorta Aneurysm | 3D | nnU-Net | 3D nnU-Net iterative training on preoperative and postoperative data. Anatomic landmarks placed for aorta sectioning. Density-based threshold for adipose tissue. PVAT analysis: Fat around aorta / aneurysm measured by HU attenuation at selected distances around aorta / aneurysm. DSC: 97.2 (test set), 97.7% (external test set) |
| Epifanov et al. [76] 2024 | CT | Lumen Thrombus Calcifications | 3D | U-Net based | 3D U-Net trained on preoperative data. ResNet-50 encoder and upsampling to decoder. Largest connected component filtration (LCF) and filling holes filtration (FHF). Spatial and intensity data augmentation. DSC: 83.12% |
| Ma et al. [65] 2023 | NCCT | Lumen Thrombus | 3D | Autoencoder | 2D Feature extracted and fused, Convolutional and CNN decoding modules. DSC: 88.7% |
| Mu et al. [66] 2023 | CTA | Lumen Thrombus | 3D | Cascade U-Net | 3D U-Nets in cascade on preoperative data. Subsampled CTA images for long-range dependencies and feature fusion and mixed pyramid pooling in the second U-Net. Overlapping 3D patches and majority class selection. Length, Surface, Volume, Max Radius, Mean Radius, Undulation Index, Tortuosity automated measurements DSC: 94.5% (Lumen) and 80.4% (ILT) |
| Jung et al. [41] 2023 | CTA | Lumen Thrombus | 2D | Bi-CLSTM Mask-RCNN | Mask-RCNN and lstm training on postoperative data. Mask-RCNN provides initial image segmentation, and Bi-LSTM is then trained on segmented images to learn 3D relations. DSC: 87.3% |
| Caradu et al. [44] 2022 | CTA | Lumen Thrombus | 2D | U-Net | U-Net trained on preoperative and postoperative data. DSC: 95% Sensitivity: 92.9% |
| Burrows et al. [27] 2022 | CECT | Lumen Thrombus Stent | 2D | Encoder-decoder VAE | VAE model trained on postoperative data. Enhanced edge detection as initial segmentation and an Encoder-Decoder. DSC: 90.9% (Thrombus), 93.7% (Stent & Lumen) |
| Wang et al. [53] 2022 | CTA | Lumen Thrombus | 2D | Transfer Learning DeepLabv3+ with ResNet-50 backbone | DeepLabv3+ segmentation on preoperative and postoperative data. Morphological feature induction. Radiomic Feature extraction and machine learning to predict severe adverse events (SAE / No SAEq) ResNet-50 feature extraction. Mean IOU 90.78% (test set), DSC: 95.16% (calculated on IOU) Accuracy: 85%, F1-score: 89% |
| Chung et al. [45] 2022 | CTA | Lumen Aneurysm Wall | 2D | U-Net | Aneurysm wall and Lumen segmentation on preoperative data using U-Net. Point cloud and surface mesh construction. Morphological feature extraction on 3D and stress prediction. Accuracy: 98% accuracy, Precision: 97.2%, Sensitivity: 96.0%, DSC: 96.59% (calculated on sensitivity,precision) |
| Wang et al. [42] 2022 | CTA | Lumen Thrombus | 2D | Transfer Learning DeepLabv3+ ResNet-50 | Aneurysm wall and Lumen segmentation on preoperative data using DeepLabv3+ with a ResNet-50 pretrain to extract features. Accuracy: 99.88%, mean BF Score: 98.29, mean IOU: 90.78% (test set), DSC: 95.16% (calculated on IOU) |
| Lareyre et al. [71] 2021 | CTA | Lumen Thrombus Spine | 2D | U-Net | Two binary U-Net classifiers were selected for lumen and spine segmentations. Thrombus segmentation using U-Net. Networks trained on top of an expert system initial segmentations with active contours for the semantics of interest. DSC: 82.66% (Lumen), 89.18% (Thrombus) |

**TABLE XIII. Data Generation techniques**

| Literature | Modality | Synthetic Modality | Method | Highlights |
|---|---|---|---|---|
| Velikova, et al. [29] 2024 | CT US | Intermediate Representation (Features) | CUT Unet | An Ultrasound Simulator generates synthetic US data features from Computed tomography ground truth. An image-to-image translation network (CUT) learns the Intermediate Representation to Ultrasound relation. Organ segmentation by U-Net is trained on Intermediate Representations. The inference process converts real US images to Intermediate Representations and subsequently performs organ segmentation. Dice Similarity Coefficient (DSC): 90.4% and 88.0% on test data. |
| Chandrashekar et al. [60] 2023 | NCCT | CTA | Cycle-GAN Con-GAN | Paired NCCT to CTA image transformation for preoperative data. Con-GAN and Cycle-GAN training. Accuracy: 86.1% (Cycle-GAN), 85.7% (Con-GAN) |
| Lyu et al. [54] 2023 | NCCT | CTA | novel GAN | Paired NCCT to CTA image transformation for preoperative data. The arhitecture includes a generator module (image synthesis, encoder-decoder), a corrector module (adapt to CTA, encoder-decoder) and a discriminator (synthesis evaluation, error estimation). Accuracy: 86%, Sensitivity: 87%,Specificity: 98% |
| Hu et al. [62] 2022 | NCCT | CECT | U-Net based GAN | Paired NCCT to CECT image transformation for preoperative data. U-Net like generator using wavelet transform modules. Lipschitz constraints to discriminator. F1-score: 85%, Precision: 79% |
| Li et al. [64] 2022 | CTA | Synthetic CTA | novel CNN | Synthetic preoperative data using CTA reconstruction. Noise free standard dose and simulated low dose images to train novel CNN and learn the noise relations of low-dose signal. An iterative minimization/optimization procedure is done which employs DL image correction, projection, comparison, high-quality data synthesis. |

### *I. COMPUTATIONAL REQUIREMENTS AND COST ANALYSIS*

In this subsection, the authors collected several factors observed in some of the studies of interest to indicate the demands of each model demands in terms of hardware resources and relevant development needs. The respective summary in Table XIV includes the execution time, the size of the model in memory or the number of trainable parameters, and the hardware that was used to perform the relative job within the declared time, together with the modality processed, the model developed and the semantics to be predicted.

Researchers note that only a minority of studies report detailed and/or accountable data on what these methods require to function. The vast majority of studies solely focus on precisely predict the entities of interest, but still its difficult to have an insight on what hardware and circumstances this method could be hosted, and thus to argue on the specific applicability concerns due to resource limits. As reported in most studies, such DL models usually use powerful CUDA enabled accelerators to train, as indicated by the respective GPU employed to all work that reports their costs, and the use of very large memory modules larger than 10GB is also preferred, which is also mandatory to most cases, considering a model size like tens of millions parameters to train on 512p 3D segments.

In addition, this cost is also relevant to the model size specifications, the input sizes, or the train methods, which introduce more complexity to accurately estimate the exact resource requirements. Even for studies that reported relevant parameters, the authors observed that quantified resource limits and reports are usually found in manuscripts. As of training and testing time reported, the methods report solutions which specifically claim to successfully handle large Imaging Volume segments instantly [11], [43] and large amount of slices per second, while all relevant methods do report short development time requirements (few hours / days).

Regarding an overall insight on the effectiveness level of distivnct techniques, the results themselves as seen in Figure 10, all tasks of interest and method categories do highlight the wide techniques that could be used towards the AAA annotation procedure. Still, the specific semantics of interest seem to remain an open challenge to optimize (like the ILT prediction), though the general effectiveness which is somewhat leveraged by a better effectiveness on predicting the "big category", results in overall metrics to be higher for the overall procedure.

### *J. QUANTIFIED QUALITY ASSESSMENT*

In this section, we reside the Risk of Bias and Applicability Concerns' visualized results in detail. Table XV presents the detailed points' of interest estimations for all studies as a traffic light plot. Within this, a green dot indicates that the relevant domain was found to positively meet any expectations set by the research community to consider a robust method as questioned within the QUADAS-II procedure. An orange dot denotes that some of the expectations' considered diverge from what was typically expected from the reviewers, or that some of the questions could not be accurately determined by this study reviewers. A red dot proposes a greater concern

**TABLE XIV. Performance Cost**

| Literature | Modality | Semantics | Method | Training Time | Testing Time | Resources & Network Size |
|---|---|---|---|---|---|---|
| Kim et al. [78] 2024 | CT | Aorta Thrombus Calcifications | 3D U-Net ensemble | Aorta: 9.5min Thrombus: 2.1min Calcifications/Vessels: 1.1min | - | NVIDIA TITAN RTX, 24,220 MiB |
| Roby et al. [55] 2025 | CTA | Lumen Outer Wall | 2D U-Net | - | $17 \pm 0.02$ ms/image 512p, saggital view | HPC cluster 2CPU,40 cores 384GB RAM 2 NVIDIA V100 |
| Wan et al. [50] 2024 | CT | Aorta | Encoder-decoder | - | - | NVIDIA RTX 4090, 24GB 84.42M params 57.71 GFLOPS |
| Zhang et al. [79] 2025 | CTA | Lumen Left / Right Renal Artery Sup. Mesenteric Artery Aneurysm | Encoder-decoder | - | - | NVIDIA V100 TENSOR CORE 91.4 GMac (FLOPs) |
| Mavridis et al. [23] 2024 | CTA | Aorta Aneurysm | U-Net | - | - | NVIDIA 4090, 24GB 4.8 M parameters |
| Lyu et al. [48] 2024 | CTA | AAA Wall | 2d U-Net ZoomNet | 5.5min+3.1min/epoch/48x512p patch | - | 2x Tesla V100,32GB 5M + 32M parameters |
| Van Praagh et al. [95] 2023 | PET/CT | Ascending aorta Aortic arch Descending aorta Abdominal aorta | 3D U-Net | - | 102–370 sec / 512p scan | NVIDIA TESLA P100, 16GB, Microsoft Azure VM |
| Spinella et al. [52] 2023 | CTA | Lumen ILT | U-Net & attention U-Net | - | Lumen: $25 \pm 1$ s/scan; Thrombus: $63 \pm 14$ s/scan Screening: $7.1 \pm 1$ min/scan | NVIDIA RTX 2080Ti |
| Mu et al. [26] 2023 | CECT | Vasculature | Cascade U-Net based | 96.02 s/epoch | - | 2x TESLA V100, 64GB 18.66M parameters |
| Ma et al. [65] 2023 | NCCT | Lumen Thrombus | Encoder-Decoder | 96.02 s/epoch | - | NVIDIA GTX1080,12GB 18.66 M parameters |
| Caradu et al. [44] 2022 | CTA | Lumen Thrombus | U-Net | - | Mean 2.5min / patient range 0.65–4.6min | - |
| Brutti et al. [37] 2022 | CTA | Lumen Thrombus | U-Net | Axial 862 Sagittal 862 Coronal 1294 Coarse 200 | 60 sec. | NVIDIA RTX 2080Ti |
| Chung et al. [45] 2022 | CTA | Lumen Thrombus | U-Net | | 20sec. end-to-end | 4x NVIDIA RTX 2080Ti |
| Lareyre et al. [71] 2021 | CTA | Lumen Thrombus Spine | U-Net based | Binary model: 2h Multilcass model: 10h | - | NVIDIA TITAN RTX |
| Fantazzini et al. [57] 2020 | CTA | Aorta | U-Net | - | $25 \pm 1$ sec./scan | NVIDIA RTX 2080Ti |
| López-Linares et al. [94] 2018 | CTA | ILT(with wall) | DetectNet modified HED network | 2h39min. | 35 img/s (Region of Interest) | Model size(HED on ROI): 56MB, 14.7M params, NVIDIA RTX 2080Ti |
| Smyrlis et al. [51] 2024 | CTA | Aorta | YOLOv9C | - | 69.45 ms/image | NVIDIA RTX 3060 27.90M params |

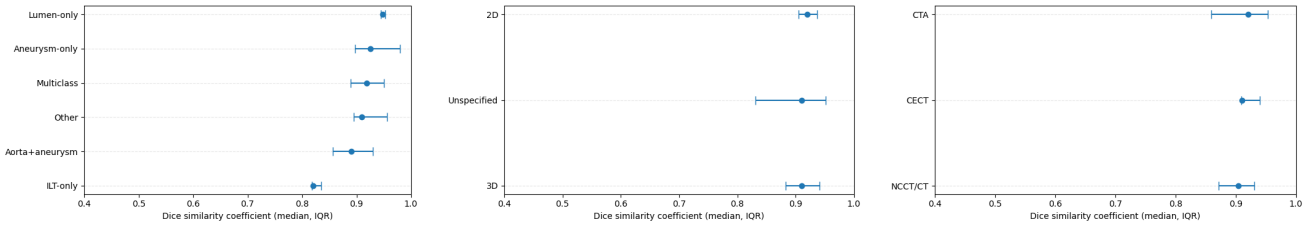


(a) Task to DSC (b) Dimension to DSC (c) Modality to DSC

**FIGURE 10. Forest plots summarizing reported DSC across segmentation pipelines. Points indicate group medians and error bars the interquartile range (IQR). (a) DSC by target semantics (task group), (b) DSC by network dimensionality (2D vs 3D), and (c) DSC by imaging modality.**

that this research may be biased or not understood as fully justified.

In order to assess how closely the methodology followed aligns with QUADAS-II checklist items, the authors consider all the relevant question set and define the level of concern for each domain for how confident was realized to be robust, according to their point of view. For the overall quality level to be determined, QUADAS-II does set the strict "any high" consideration, so the authors using this prototype attempt to highlight points of interest that each methodology could align. In general, nearly all studies found were labeled as "Unclear" or "High" in at least one or more domains. All studies do employ experimental methods, and the domain that was found to raise the least concerns was the "Reference Standard" regarding the methods' applicability. Nearly all AI-Assisted pipelines were considered to show a fair potential to be applied in industry, and nearly all researchers included in the study were understood to argue on novel optimizations towards building an automated AI-Assisted method to delineate the annotation of the AAA region and quantification of the findings. On the other hand, when discussing the same domain risk of bias, the concern level increased slightly. The methods themselves were overally considered as fine, with respect to the divergence on what each research team tries to address using the specific AI model, and only a 5% of them was observed not to fully justify its considerations.

When talking of the Index Test, a total of 23% of studies were not found to fully report the Index test criteria, while 8% of them were considered to raise greater concerns about the AI model induction process. When it comes to applicability, the vast majority of the research studies (82%) was found to comply on high applicability standards, thus being able to participate to a such automated Decision Support schema, with respect to the AI inaccuracy, which itself triggers large research discussion and experiments, due to the open-problem nature of the Segmentation, Detection, Classification and relevant tasks for their precision optimization. However, the AAA AI models discussed in this study were found to fundamentally argue on a good potential and the respective reported DSCs are often observed to reach> =90%. Most concerns in literature were spotted to the Patient Selection methods, where almost half of the studies were not found to broadly include all circumstances of interest to build their models, with respect to the task they try solve.

The respective summaries are shown in Table 11 for the Risk of Bias Concerns and Table 12 for the applicability Questions.

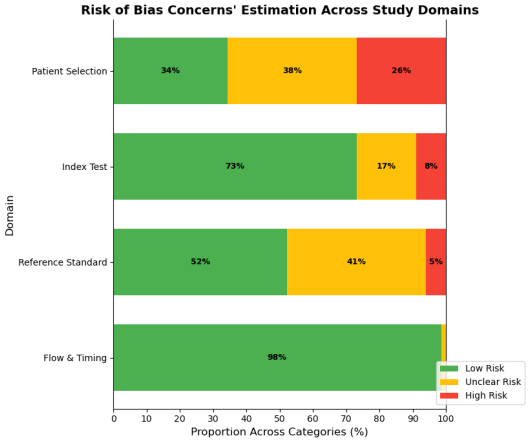


**FIGURE 11. Risk of Bias Concerns' summary with respect to Quadas II evaluation principles**

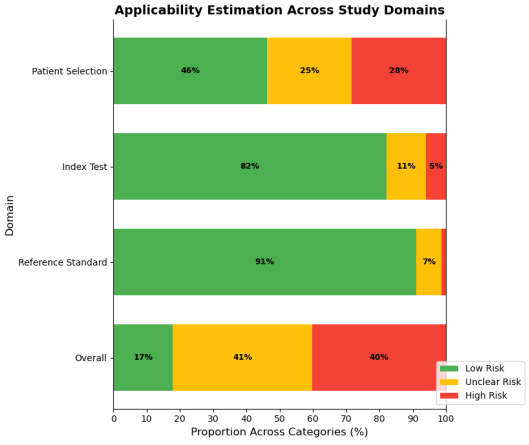


**FIGURE 12. Applicability Concerns' summary with respect to Quadas II evaluation principles**

## V. DISCUSSION

This section provides a summary of the current state of DL applications for the diagnosis and management of AAA and how it should be performed, based on the findings of the present review. Emphasis is placed on the types of tasks addressed, the evolution of DL methodologies, and the nature of the datasets used throughout the literature. A comparative analysis with previous reviews, summarized in Table XVI, is also included to contextualize our approach in relation to existing work. In doing so, this discussion aims to situate the reviewed studies within the broader research landscape and outline emerging directions in the field.

In contrast to earlier reviews identified in our screening process—many of which focused narrowly on segmentation or employed outdated DL techniques—this study incorporates literature published up to early 2025, reflecting cutting-edge developments such as transformer-based architectures and multimodal fusion approaches. Moreover, this review adheres strictly to the PRISMA methodology, with 1002 records initially identified and screened through a multiphase selection process guided by predefined exclusion criteria. This level of procedural transparency and methodological rigor, which is seldom observed in prior reviews, enhances reproducibility and mitigates the risk of selection bias. Earlier reviews often lacked clear eligibility criteria or merged disparate types of study (e.g., combining biomechanical sim-

**TABLE XV. Quadas II - Risk of Bias and Applicability Concerns**

| | Risk of Bias | | | | Applicability | | | |
|---|---|---|---|---|---|---|---|---|
| Author | Patient Selection | Index Test | Reference Standard | Timing and Flow | Patient Selection | Index Test | Reference Standard | Overall |
| Kim et al., 2024 [78] | 🟢 | 🟢 | 🟢 | 🟢 | 🟢 | 🟢 | 🟢 | 🟢 |
| Ginzburg et al., 2024 [96] | 🟢 | 🟢 | 🟢 | 🟢 | 🟢 | 🟢 | 🟢 | 🟢 |
| Roby et al., 2025 [55] | 🟡 | 🟢 | 🟢 | 🟢 | 🟡 | 🟡 | 🟢 | 🟡 |
| Wan et al., 2024 [50] | 🔴 | 🟡 | 🟢 | 🟢 | 🔴 | 🟡 | 🟢 | 🔴 |
| Zhang et al., 2025 [79] | 🟡 | 🔴 | 🟢 | 🟢 | 🟡 | 🔴 | 🟢 | 🔴 |
| Mavridis et al., 2024 [23] | 🟢 | 🟢 | 🟡 | 🟡 | 🟢 | 🟢 | 🟢 | 🟡 |
| Zhang et al., 2024 [59] | 🔴 | 🔴 | 🔴 | 🟢 | 🔴 | 🔴 | 🟡 | 🔴 |
| Lyu et al., 2024 [48] | 🔴 | 🟢 | 🟢 | 🟢 | 🟡 | 🟢 | 🟢 | 🔴 |
| Postiglione et al., 2024 [74] | 🟢 | 🟡 | 🟢 | 🟢 | 🟢 | 🟢 | 🟢 | 🟡 |
| van Praagh et al., 2024 [95] | 🟡 | 🟡 | 🟢 | 🟢 | 🟢 | 🟢 | 🟢 | 🟡 |
| Epifanov et al., 2024 [76] | 🟡 | 🟢 | 🟢 | 🟢 | 🟡 | 🟢 | 🟢 | 🟡 |
| Chatterjee et al., 2024[28] | 🟡 | 🟡 | 🟢 | 🟢 | 🟡 | 🟢 | 🟢 | 🟡 |
| Velikova et al., 2024 [29] | 🟡 | 🟡 | 🟡 | 🟢 | 🔴 | 🟡 | 🟢 | 🔴 |
| Ma et al., 2024[92] | 🟡 | 🟡 | 🔴 | 🟢 | 🟡 | 🟡 | 🔴 | 🔴 |
| Hassan et al., 2024 [25] | 🟡 | 🟡 | 🟢 | 🟢 | 🟡 | 🟢 | 🟢 | 🟡 |
| Spinella et al., 2023[52] | 🟡 | 🟡 | 🟢 | 🟢 | 🟡 | 🟡 | 🟢 | 🟡 |
| Borisova et al., 2023 [36] | 🟢 | 🟢 | 🟢 | 🟢 | 🟢 | 🟢 | 🟢 | 🟢 |
| Mu et al., 2023 [26] | 🟡 | 🟢 | 🟢 | 🟢 | 🟡 | 🟢 | 🟢 | 🟡 |
| Ma et al., 2023 [65] | 🔴 | 🔴 | 🟢 | 🟢 | 🟡 | 🟡 | 🟢 | 🔴 |
| Mu et al., 2023 [66] | 🔴 | 🟢 | 🟢 | 🟢 | 🔴 | 🟢 | 🟢 | 🔴 |
| Chandrashekar et al., 2023 [60] | 🟡 | 🟢 | 🟡 | 🟢 | 🟡 | 🟢 | 🟡 | 🟡 |
| Lyu et al., 2023[54] | 🟢 | 🟢 | 🟡 | 🟢 | 🟢 | 🟢 | 🟢 | 🟡 |
| Wang et al., 2023 [40] | 🟢 | 🟢 | 🟢 | 🟢 | 🟢 | 🟢 | 🟢 | 🟢 |
| Jung et al., 2023 [41] | 🟡 | 🟢 | 🔴 | 🟢 | 🟢 | 🟢 | 🟡 | 🔴 |
| Saleem Javeed et al., 2023 [30] | 🔴 | 🔴 | 🟡 | 🟢 | 🔴 | 🔴 | 🟢 | 🔴 |
| Zhang et al., 2023 [84] | 🔴 | 🟡 | 🟡 | 🟢 | 🔴 | 🟢 | 🟢 | 🔴 |
| Tomihama et al., 2023 [80] | 🟢 | 🔴 | 🟡 | 🟢 | 🟢 | 🔴 | 🟡 | 🔴 |
| Abdolmanafi et al., 2023 [32] | 🟢 | 🟢 | 🟢 | 🟢 | 🟢 | 🟢 | 🟢 | 🟢 |
| Chandrashekar et al., 2022 [93] | 🟡 | 🟢 | 🟢 | 🟢 | 🟢 | 🟢 | 🟢 | 🟡 |
| Caradu et al., 2022 [44] | 🟢 | 🟢 | 🟡 | 🟢 | 🟢 | 🟢 | 🟢 | 🟡 |
| Burrows et al., 2022 [27] | 🟡 | 🟢 | 🟡 | 🟢 | 🟡 | 🟢 | 🟢 | 🟡 |
| Brutti et al., 2022 [37] | 🟡 | 🟢 | 🟢 | 🟢 | 🟢 | 🟢 | 🟢 | 🟡 |
| Wang et al., 2022 [53] | 🟡 | 🟢 | 🟢 | 🟢 | 🟢 | 🟢 | 🟢 | 🟡 |
| Chung et al., 2022 [45] | 🔴 | 🟢 | 🟢 | 🟢 | 🔴 | 🟢 | 🟢 | 🔴 |
| Wang et al., 2022 [42] | 🟡 | 🟢 | 🟡 | 🟢 | 🟢 | 🟢 | 🟢 | 🟡 |
| Miao et al., 2022 [56] | 🔴 | 🔴 | 🟡 | 🟢 | 🟡 | 🟢 | 🟢 | 🔴 |
| Kongrat et al., 2022 [63] | 🟢 | 🟡 | 🟡 | 🟢 | 🔴 | 🟡 | 🟢 | 🔴 |
| Hwang et al., 2022 [69] | 🟢 | 🟢 | 🟢 | 🟢 | 🟢 | 🟢 | 🟢 | 🟢 |
| Siriapisith et al., 2022 [81] | 🟢 | 🟢 | 🟢 | 🟢 | 🟢 | 🟢 | 🟢 | 🟢 |
| Salvi et al., 2022 [61] | 🟢 | 🟢 | 🟡 | 🟢 | 🟢 | 🟡 | 🟢 | 🟡 |
| Dziubich et al., 2021[46] | 🟢 | 🟢 | 🟢 | 🟢 | 🟢 | 🟢 | 🟢 | 🟢 |
| Golla et al., 2021 [85] | 🟢 | 🟢 | 🟢 | 🟢 | 🟢 | 🟢 | 🟢 | 🟢 |
| Hu et al., 2022 [62] | 🟡 | 🟢 | 🟢 | 🟢 | 🟡 | 🟢 | 🟢 | 🟡 |
| Lareyre et al., 2021 [71] | 🟢 | 🟢 | 🟡 | 🟢 | 🟢 | 🟢 | 🟢 | 🟡 |
| Zheng et al., 2021 [47] | 🔴 | 🟡 | 🟡 | 🟢 | 🔴 | 🟢 | 🟢 | 🔴 |
| Zheng et al., 2019 [38] | 🔴 | 🟡 | 🟡 | 🟢 | 🔴 | 🟢 | 🟢 | 🔴 |
| Mohammadi et al., 2019 [70] | 🔴 | 🟢 | 🟡 | 🟢 | 🔴 | 🟢 | 🟢 | 🔴 |
| Hahn et al., 2019 [35] | 🔴 | 🟢 | 🟢 | 🟢 | 🟢 | 🟢 | 🟢 | 🔴 |
| Dziubich et al., 2020 [39] | 🔴 | 🟢 | 🟡 | 🟢 | 🔴 | 🟢 | 🟢 | 🔴 |
| Habijan et al., 2020 [31] | 🟡 | 🟢 | 🟡 | 🟢 | 🔴 | 🟢 | 🟢 | 🔴 |
| Hahn et al., 2020 [58] | 🟢 | 🟢 | 🟢 | 🟢 | 🟡 | 🟢 | 🟢 | 🟡 |
| Fantazzini et al., 2020 [57] | 🟡 | 🟢 | 🟡 | 🟢 | 🟢 | 🟢 | 🟢 | 🟡 |
| Hong & Sheikh, 2016 [33] | 🔴 | 🟢 | 🔴 | 🟢 | 🔴 | 🟢 | 🟡 | 🔴 |
| Lopez-Linares et al., 2018 [43] | 🟡 | 🟢 | 🟡 | 🟢 | 🟡 | 🟢 | 🟢 | 🟡 |
| López-Linares et al., 2018 [94] | 🟢 | 🟢 | 🟢 | 🟢 | 🟢 | 🟢 | 🟢 | 🟢 |
| López-Linares et al., 2019 [75] | 🟡 | 🟢 | 🟡 | 🟢 | 🟢 | 🟢 | 🟢 | 🟡 |
| Lu et al., 2019 [82] | 🟡 | 🟢 | 🟢 | 🟢 | 🟢 | 🟢 | 🟢 | 🟡 |
| López-Linares et al., 2017 [73] | 🟡 | 🟢 | 🟡 | 🟢 | 🟢 | 🟢 | 🟢 | 🟡 |
| Salvi et al., 2021 [67] | 🟡 | 🟢 | 🟡 | 🟢 | 🔴 | 🟢 | 🟢 | 🔴 |
| Koçer et al., 2024 [83] | 🟡 | 🟢 | 🟡 | 🟢 | 🔴 | 🟢 | 🟢 | 🔴 |
| Smyrlis et al., 2024 [51] | 🔴 | 🟢 | 🟢 | 🟢 | 🔴 | 🟢 | 🟢 | 🔴 |
| Benčević et al., 2022 [24] | 🔴 | 🟢 | 🟡 | 🟢 | 🔴 | 🟢 | 🟢 | 🔴 |
| Rajmohan et al., 2024 [72] | 🔴 | 🟢 | 🟡 | 🟢 | 🔴 | 🟢 | 🟢 | 🔴 |
| López-Linares et al., 2018 [94] | 🟢 | 🟢 | 🟢 | 🟢 | 🟢 | 🟢 | 🟢 | 🟢 |
| Camara et al., 2022 [49] | 🟢 | 🟢 | 🟡 | 🟢 | 🟢 | 🟢 | 🟢 | 🟡 |
| Li et al., 2022 [64] | 🟢 | 🟢 | 🟢 | 🟢 | 🟡 | 🟢 | 🟢 | 🟡 |
| Adam et al., 2021 [77] | 🟢 | 🟢 | 🟢 | 🟢 | 🟢 | 🟢 | 🟢 | 🟢 |

ulations with image-based diagnostics) without appropriate stratification, thereby reducing interpretability.

The current literature reveals a wide research landscape that includes all known DL basic tasks. A substantial proportion of studies focus on image segmentation, particularly of the aneurysmal sac, intraluminal thrombus (ILT) and adjacent anatomical structures, using CT or CTA. Although segmentation remains a core task, comparatively fewer studies have been found to address classification, rupture risk prediction, or comprehensive clinical decision-support systems. In fact, the classification task is also implied in the downstream detection and segmentation efforts, where some logic is also employed to determine the label of an entity of interest (from region of interest to pixel, respectively). Subsequently, within the segmentation task, distinct approaches were found to annotate a number of semantics (multiclass segmentation for aorta, thrombus, and others), a single semantic (aorta segmentation including any thrombus), and Region of Interest segmentation methods, which segment a sub-region of the image as soon as a detection model spot an aneurysm instance.

In particular, most DL models have been developed using single-center retrospective datasets with limited sample sizes and minimal external validation, often relying on in-house institutional data. This could question the generalizability and reproducibility of the findings and their actual scalability in-the-wild, when real-world conditions shall impose significant instance variations, for example various-sized ILT and calcifications. In addition, comorbidities such as fat presence or other pathological findings that may be present in a CTA capture and the patient's history, such as a different disease that coexists, or signs of previous surgery.

Most of the research discussed in this review focuses on preoperative planning and early detection of AAA in CTA. Only a few studies are specialized on postoperative screening (8 works), while another 10 studies involve preoperative and postoperative data. Since postoperative data can present additional objects of interest to be detected/segmented, the entire AAA detection and delineation landscape requires extra data and effort to be done for modeling, in order to learn object cases like stent grafts[40].

Current research focuses on advanced architectures including attention mechanisms and 3D convolutional networks, yet the field lacks standardized benchmarks together with open-access datasets, which would enable fair model comparison and collaborative development. This systematic review reveals that DL applications for AAA imaging use single-center retrospective data sets that lack diversity and/or expert validation. The lack of standardized protocols across imaging methods, along with processing pipelines and annotation approaches, creates challenges for meaningful result comparisons. For example, many different taxonomies of interest are observed across studies, often containing differently defined classes of interest and number of semantics. Usually, the aorta entity is distinguished with or without the ILT, while only a few other entities are yet modeled (calcifications or fat). In fact, for the entire image segmentation, only two studies address calcification detection in modeling [78], [76], while in Region of Interest segmentation only one [32].

However, the definition of the exact boundary of each entity could differ from study to study. Thus, the results' comparison cannot always be straightforward, although the exact visual definition of each entity of interest could be questioned with respect to the ability of the models to distinguish it. In case of semantic segmentation for ILT, acceptable definitions could include the entire aorta wall, or just the additional thrombus made. Or, the calcifications together with the aorta wall and separately. Most studies yet experiment with one or two classes at most and usually model a distinct aorta and ILT entity.

As for DL architecture designs, researchers on AAA recent segmentation methods have mainly trusted the U-Net schema to build their models on top, or as a first choice option Figure 13 depicts this distribution, where 20 studies were observed to involve U-Net as a first choice solution, while 10 aggregate the usage of some other design. Within this concept, sophisticated variations have been proposed, even involving signal processing methods and the frequency domain [26], or data fusing object coordinate information in the model[81], to enhance the model precision. The descent performance of this schema is open to further research, while other architectures presenting promising success in early experimental stages[51], are also open to further study for their applicability on the AAA delineation task. Likewise, the novel architecture designs involving the traditional convolution and the recent attention mechanisms may also provide descent model proposals for AAA DL modeling.

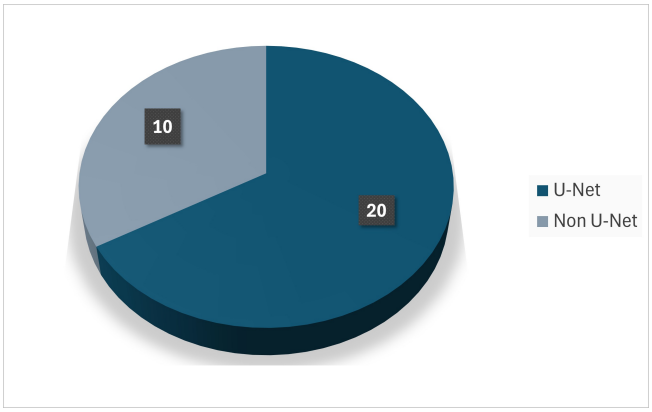


**FIGURE 13.** **Architecture of the proposed approaches**

The path forward also demands standardized evaluation frameworks together with larger publicly available datasets that include transparent reporting of data processing and computational resources. A curated and openly accessible "golden dataset" would establish a major milestone which enables consistent evaluation of algorithms through a shared benchmark. The clinical adoption of models depends on both

interpretability and compliance with regulatory standards to achieve safe and effective use in healthcare settings.

### A. LIMITATIONS OF INCLUDED STUDIES

The beneficial utility of the included studies is impacted by a number of limitations, notwithstanding the encouraging advancements found. First, most studies are primarily based on single-center retrospective data sets, which are typically obtained from homogeneous groups. This limits the scope of generalizing results and applying models to heterogeneous clinical settings, while the model scalability in-the-wild is questionable to perform in the presence of real world conditions, where the unseen data variability significantly increase.

Furthermore, despite the extensive usage of cross-validation evaluation in the vast majority of studies, further structured risk-of-bias evaluation tools were limited in the included studies. These tools help to precisely infer internal validity, define likely sources of bias, and accurately quantify methodological quality. Moreover, external validation was rarely performed. Most of the studies only measured model performance on internal test sets. Similarly, few papers provided uncertainty estimation (e.g. confidence intervals), limiting the models from application in clinical decision support where robustness and interpretability are required.

In addition, annotation protocols varied considerably. Most ground truths were based on single-expert manually segmented data, with unstated inter-rater reliability. This introduces subjectivity and limits the comparability of evaluation metrics across studies. Due to the variably posed class definition and the evaluation protocols, the ability to straightforwardly compare distinct models is limited, namely, across every segmentation method to its likewise models. Finally, the lack of statistical synthesis, for example meta-analysis or effect size comparisons, limits the quantitative comparison of overall performance trends. The significant variations in evaluation protocol, preprocessing, and outcome definitions accross studies significantly limits the ability to make extensive straightforward quantitative comparisons.

### B. COMPARATIVE ANALYSIS WITH PRIOR REVIEWS

In order to situate this review in the current literature, it is important to compare it to the previous efforts in venturing into DL-based applications in AAA imaging. This comparison enables us to identify methodological excellence, shared loopholes, and shifting trends in architectural design, application of datasets, and clinical focus. This section outlines how our review builds upon previous work through a more complete and systematic synthesis of the field.

Among the related works, Raffort et al. [98] provided one of the earliest overviews of artificial intelligence in AAA, analyzing more than 9,900 CT scans. While their review highlighted early advances in segmentation and risk stratification, it lacked a structured methodological framework such as PRISMA. Similarly, the works by Lareyre et al. [99] and Baek et al. [99] offered narrative reviews on segmentation techniques and translational potential but did not undertake a systematic evaluation of model quality or study design, thereby limiting reproducibility and bias assessment.

In contrast, Kodenko et al. [100] employed a PRISMA-guided methodology in their systematic review of eight studies focused on opportunistic AAA screening in routine CT imaging. While their structured approach marked a methodological advance, the review primarily assessed diagnostic accuracy and did not delve into architectural comparisons or data quality appraisal.

More recent contributions, such as those by Huang et al. [14] and Wang et al. [101], [102], emphasize the potential of DL models—including U-Net, nnU-Net, and CNN variants—for segmentation and large-scale AAA screening. However, these studies remain narrative in form and omit key elements such as bias assessments, protocol registration, or reproducibility evaluation.

This systematic review presents a focused and up-to-date synthesis of recent advances in DL methods for AAA diagnosis, segmentation, and management. Several distinct methodological and analytical characteristics distinguish this work from prior reviews, presented in Table XVI

Initially, the thematic scope is precisely delimited. Unlike previous reviews that group together aneurysms of varying anatomical regions or include multiple cardiovascular disorders, this review focuses exclusively on AAAs and image-based DL applications on advanced tomographic modalities such as CT, CTA, and MRI (Section II-B). Ultrasound and simulation-based studies were excluded to ensure clinical relevance and high spatial fidelity.

In addition, this study adheres rigorously to the PRISMA framework, implementing a transparent and reproducible methodology. From an initial pool of 1,921 retrieved records, peer-reviewed studies were ultimately included, with well-defined eligibility criteria applied across multiple databases (see Figure 1). In contrast, many earlier reviews lack clarity regarding selection flow, screening tools, or exclusion rationale (Table XVI) [99], [103], [14], [100], [101], [102].

It is also noteworthy that a significant number of previous contributions take the form of narrative reviews [99], [103], [14], which, while often insightful, lack systematic coverage or transparency in selection criteria. In contrast, only a few systematic reviews have been published to date [100], [101], [102], and most include relatively limited numbers of studies, often fewer than 20, highlighting a gap in comprehensive and methodologically robust synthesis efforts.

Moreover, the coverage of the literature in this review spans an entire decade (2015–2025) (Table I), capturing not only conventional CNN architectures, but also newer transformer-based and hybrid models such as TransUNet. These recent developments are largely overlooked in previous surveys, which typically emphasize early convolutional models while neglecting architectural innovation and hybrid attention mechanisms.

Another key strength lies in the structured dual-layer taxonomy adopted for literature analysis. Studies are categorized both by DL task—classification, detection, segmenta-

**TABLE XVI. Review works on decision support for Abdominal Aortic Aneurysm**

| Literature | Title | Type of Review | Year | Included Papers | Covered Study Period | Key Research Findings |
|---|---|---|---|---|---|---|
| Raffort et al.[98] | Artificial Intelligence in Abdominal Aortic Aneurysm: A Systematic Review | Systematic | 2019 | 34 | May 2019 – January 2000 | AI improves AAA image segmentation, growth and rupture risk prediction, and preoperative planning. It supports personalized treatment and enhances postoperative outcome evaluation. |
| Baek et al.[99] | Current state-of-the-art and utilities of machine learning for detection, monitoring, growth prediction, rupture risk assessment, and post-surgical management of abdominal aortic aneurysms | Narrative | 2022 | 11 | Not specified | The study highlights the need for improved AAA management through personalized strategies. It discusses the RAW index for rupture risk, EVAR/OSR outcomes, and how patient-specific biomechanical factors can guide prediction and intervention. |
| Kodenko et al.[100] | Diagnostic accuracy of AI for opportunistic screening of abdominal aortic aneurysm in CT: A systematic review and narrative synthesis | Systematic | 2022 | 8 | Not Specified | The review assessed AI methods for AAA detection in noncontrast CT, reporting high sensitivity (95%), specificity (96.6%), and Dice score (0.96). However, study heterogeneity and unbalanced datasets raise concerns, indicating a need for standardized, robust validations. |
| Sokol & Nguyen[103] | Risk prediction for abdominal aortic aneurysm: One size does not necessarily fit all | Narrative | 2023 | 12 | Not Specified | This work emphasizes the limitations of size-based AAA diagnosis and advocates for personalized strategies using ML and molecular imaging. It highlights demographic disparities, especially underdiagnosis in women, and calls for inclusive clinical trials and broader risk assessment models. |
| Huang et al.[14] | Deep learning techniques for imaging diagnosis and treatment of aortic aneurysm | Narrative | 2024 | 23 | Not specified | Deep learning improves AA imaging accuracy and treatment planning. Models like ResNet and U-Net support lesion segmentation and stent prediction. The study highlights clinical benefits and research gaps. |
| Wang et al.[101] | Deep Learning Models for Aorta Segmentation in Computed Tomography Images: A Systematic Review And Meta-Analysis | Systematic | 2024 | 16 | Up to March 2024 | This systematic review found DL models highly effective for aorta segmentation in CT, with a pooled Dice score of 96%. It highlights geographic performance variation, limited use of cross-validation, and moderate reporting quality. DL is shown to support accurate and standardized cardiovascular diagnosis. |
| Wang et al.[102] | The role of deep learning in aortic aneurysm segmentation and detection from CT scans: A systematic review and meta-analysis | Systematic | 2024 | 17 | 2020–2024 | This meta-analysis found DL models achieved 96% sensitivity and 97% specificity for AA detection, with a Dice score of 94% for segmentation. Performance varied by region, and larger training datasets improved accuracy. DL integration may enhance early diagnosis and outcomes. |
| **This Work** | **Decision support on Abdominal Aortic Aneurysm with Deep Learning on Advanced Imaging techniques: A Systematic Literature Review** | **Systematic** | **2025** | **68** | **2015–2025** | **Comprehensive summary of deep learning approaches applied to CT and MRI data for abdominal aortic aneurysm; covers automated detection, image processing, segmentation, and quantification to support diagnosis, monitoring, and treatment planning.** |

tion, forecasting, and data generation—and by the specific anatomical targets modeled (e.g., lumen, intraluminal thrombus, aortic wall, calcifications). This categorization provides clinically meaningful insights and supports a more targeted interpretation of model performance (Tables V–IV).

Equally important is the emphasis on translational relevance. Only studies based on real patient-derived imaging data were included, with synthetic, animal, and purely simulation-based approaches excluded (Section II-C). The review also highlights the disproportionate reliance on private datasets, underscoring current barriers to reproducibility and external validation (see Figure 3).

Two systematic reviews published in 2024 by Wang et al. [101], [102] deserve closer scrutiny. Despite sharing similar themes and timelines, these works refer to substantially different sets of primary studies. Several relevant papers included here are entirely omitted from both reviews, despite thematic alignment. This inconsistency raises concerns regarding the comprehensiveness and methodological transparency of their search strategies.

Furthermore, the inclusion logic applied across both Wang reviews appears ambiguous. While one nominally targets aortic segmentation from CT [101] and the other focuses on aneurysm detection [102], several studies that fit both categories are omitted from both. No use of PRISMA flowcharts, detailed exclusion criteria, or bias assessments is reported. Architectural stratification is minimal, with no mention of post-2022 models such as YOLOv9 or attention-enhanced segmentation frameworks.

Additionally, both reviews restrict their scope to CT imaging and ignore contributions based on CTA, CECT, or hybrid modalities. This limitation narrows the clinical applicability, especially in the context of preoperative planning and follow-up scenarios, where CTA remains the gold standard. No discussion is offered regarding postoperative AAA management or multi-stage modeling.

Finally, a comparison of coverage (Table XVI) illustrates that each Wang review includes fewer than 20 studies, while this review synthesizes works covering all the major DL tasks and stages of the disease. The broader scope, methodological rigor, and greater granularity presented here offer a more accurate, actionable, and timely perspective on DL's evolving role in AAA decision support.

### C. FUTURE OF THE RESEARCH

Future directions in AAA research are increasingly shaped by the convergence of DL, clinical needs, and data-driven precision medicine and treatment. A key priority is the creation and open distribution of large, multicenter, and demographically diverse datasets that reflect the heterogeneity of clinical practice in terms of imaging protocols, patient demographics, and pathology. This is crucial to overcome barriers related to data availability and privacy, as well as institutional constraints that often limit data sharing. Managing these challenges will require standardized frameworks for data quality, storage, and analysis, along with robust policies for privacy protection.

Interdisciplinary collaboration is essential to advance these efforts. Partnerships between clinicians, biomedical informat-

ics researchers, and technical experts can accelerate translational research and bridge the gap between algorithm development and clinical implementation.

At the modeling level, future research must prioritize the development of explainable DL models. Traditional "black-box" systems are increasingly being further understood and enhanced by transparent models incorporating features such as saliency maps and uncertainty estimation. Not only do these tools enhance interpretability for programmers, but also support clinician-in-the-loop workflows, increasing trust, and facilitating real-world adoption and scalability.

Recent technological advances for DL allow the integration of imaging data with additional patient-specific information, including electronic health records, genomic profiles, and biomechanical simulations, to enable personalized risk stratification and tailored management strategies in advanced decision support systems. The use of advanced architectures for intelligent modeling shall further improve the precision and generalizability of the predictive ability on the distinct subtasks involved. The invention and development of more accurate DL methods on the predictive tasks of interest remain an open research field for novel techniques to be designed on top of the convolution and attention operations to improve the predictive capability for the classes of interest.

To the time being, the experimental works' results do allow to build sophisticated Decision Support pipelines, presenting reasonable precision in documents (DSC over 90%), thus making it possible for this pathology to apply on a reduced risk of bias. Although, a relevant concern is still raised due to the natural inaccuracy of AI and open-problem condition to the algorithm optimization direction in order for this research to deploy. To this purpose to meet, the medical community standards propose for a broad range of circumstances to predict, implying relevant data availability and cooperation needs.

In the meantime, the AAA problem definition shall be further researched on the classes of interest which can be precisely learned for the DL models to result in better annotations. In addition, the wider inclusion of more AAA-related semantics for the modeling and experimental procedures (such as calcifications and fat) shall provide more detailed visual and quantitative representations to the decision-support approaches, while the requirement for accurate modeling poses an open research challenge. In the AAA cases, some of the classes of major medical interest are still supported by non DL procedures for visual annotation. Though these algorithms still present a relevant prediction error and an open-problem challenge, the authors consider the modelling interest as a whole as an open challenge.

Regarding the DL architectures themselves, although recent U-Net schema models have yet presented remarkable precision clues, research on DL architecture designs remains open to improvements on top of this architecture or introducing novel ones, while the AAA problem still poses significant learning challenges for the segmentation task, the taxonomy of interest, and the actual entities of interest that are finally detected by models to be included (e.g. calcifications). Although segmentation and classification tasks have shown substantial progress, applications of DL in quantitative measurement and rupture risk prediction remain underdeveloped. Future studies may focus on clinically validated longitudinal models capable of capturing the dynamic progression of AAA and supporting continuous monitoring.

Lastly, the field must commit to transparent evaluation practices. Standardized reporting of computational resources, validation protocols, and benchmarking on open datasets will be necessary to ensure comparability, methodological rigor, and clinical relevance. Regarding the reportings performed in studies of interest, the authors consider the vast majority of studies to reasonably justify any AI-modeling and propose interesting novelties on a descent precision, which is also proposed by the fact that when inducting the relevant metrics into a single (like DSC in this study), the authors can still observe descent precision in studies overall. However, a common comparability nomenclature, which yet commonly exists to the distinct AI tasks (advanced metrics that justify the AI modeling itself, like DSC), could also further expand to biomedical research community.

As of the resource reportings, all relevant studies that were observed did report the use of recent CUDA enabled accelerators with a large memory capacity, which is a reasonable need to AI Training procedures, and also timely accomplishment time to run. Testing phase reportings in a minority of studies also suggest a descent performance to handle such large volumetric data. Besides, a richer reportings' protocol including more system requirements' insight could even clearer facilitate more applicability questionings on automated decision support as a service, and may further highlight the potential of any method to fit or apply on candidate devices and recent technology. However, from the authors point of view, the pipelines themselves, as seen in the quality assessment discussion (QUADAS-II), were widely capable of giving positive answers to established signaling questions.

Together, these trends point to a future where AI-powered AAA tools are more collaborative, interpretable, personalized, and robust - ultimately improving both research outcomes and patient care.

## VI. CONCLUSION

This systematic review highlights the significant progress made over the past decade in applying DL techniques to the diagnosis, segmentation, and management of AAA using advanced imaging modalities such as CT, CTA, and, to a lesser extent, MRI. A total of studies published between 2015 and early 2025 were included, providing a comprehensive overview of the evolving methodologies and clinical relevance of DL approaches for AAA assessment.

The review demonstrates that segmentation remains the most prevalent application of DL in AAA research, with 40 studies focused on delineating structures such as the aorta lumen, intraluminal thrombus (ILT), calcifications, and the

outer aortic wall (Table IV, Table IX, Table X). U-Net and its variants (e.g. 2D U-Net, 3D U-Net, Attention U-Net, nnU-Net) were the dominant architectures, achieving consistently high segmentation accuracy. For example, Roby et al. [55] reported a DSC over 95% for aortic segmentation and two distinct classes, while Kim et al. [78], an ensemble U-Net model, achieved over 92.5% performance (DSC) for aorta and thrombus, while additionally addressing calcification detection.

Despite promising performance metrics, several challenges hinder the clinical translation of these models. Data limitations remain a major concern. Most of the studies used individual center-based in-house datasets ($n = 57$), with only 7 studies entirely using open datasets (Figure 3, Table II). This limits any external validation possibility. Furthermore, the findings reveal that MRI-based studies are notably underrepresented, despite the advantages of MRI in soft tissue characterization and non-ionizing radiation. The findings reveal that CTA is the preferred standard for early and accurate screening, as a fast and affordable method to accurately capture the presence of AAA.

Another notable improvement refers to the interpretability and transparency in DL systems. Most models function as black boxes, without offering explainable outputs to researchers, or to facilitate clinical decision-making in vascular care workflows and enhance screening. Furthermore, only 13 out of studies integrate into the quantification of any finding, such as aneurysm diameter or thrombus volume, and less than a third were found to report computational cost data, limiting evaluations of scalability and clinical feasibility.

In terms of DL tasks, while segmentation was most seen, classification (8 studies) and detection (3 studies) of AAA were also explored, often using transfer learning with architectures such as ResNet, DenseNet, and EfficientNet (Table VII, Table VIII). However, only one study addressed forecasting on the aneurysm evolution and five studies worked on data generation, highlighting less interest in rupture risk prediction and synthetic data generation respectively, with DL on CTA and MRI modalities and the tasks defined(Table V).

This work attempts to pose a strict PRISMA-based methodology and a narrower focus on AAA-specific, imaging-based DL applications, with likewise researches, such as Raffort et al.[98], Lareyre et al., or Kodenko et al.[100], to study a relaxed range of differing fields. This work filters for image-based AAA studies using actual patient data for DL on CT, CTA, or MRI (Table XVI), excluding any work on simulation, biomechanics, and other imaging modalities.

To facilitate the clinical translation of DL models for AAA diagnosis and management, several critical directions for future research emerge from this review. First, the development and open availability of large-scale, multicenter datasets should be prioritized to facilitate model generalizability and enable robust external validation, able to reflect the variability of real-world imaging protocols, patient populations, and conditions.

Furthermore, future work could improve the interpretability of DL models, incorporating explainable AI mechanisms to foster clinical trust and provide transparency in decision making, particularly in scenarios involving surgical planning and rupture risk assessment. In addition, integration of imaging-based outputs and complementary patient-level data, such as electronic health records, genetic information, and biomechanical simulations into advanced DSS could support a more comprehensive and personalized approach to disease assessment.

Moreover, while substantial progress is observed on the segmentation task, further research could integrate robust automated quantification techniques and longitudinal analysis. Current studies seldom address AAA growth monitoring or rupture prediction areas to improve treatment outcomes. DL models tackling these predictive tasks along with quantification methods could be evaluated on longer-term clinical timelines. In addition, further research could provide additional results on the semantics of interest that could be annotated on such imaging methods, including a wider range of comorbidities and AAA-related pathology, such as fat presence and detection of calcification.

Lastly, the field would benefit from standardized benchmarking protocols and evaluation frameworks to allow fair comparison between studies and promote scalability to real-world conditions in the wild. Open-source implementations, validation challenges, and cross-institutional collaborations can drive innovation and facilitate the integration of research into clinical tools.

In general, this review underscores the considerable potential of DL in improving AAA management, while also illuminating the methodological and practical challenges that remain. To the authors' considerations, the transition from experimental prototypes to reliable, deployable systems and advanced patient care could benefit by addressing the above remarks.

## AUTHOR CONTRIBUTIONS

In this paragraph, we acknowledge the authors separate work contribution for this work to be accomplished. Below, we denote the authors' distinct roles according to the CRediT[104] taxonomy:

**Conceptualization**: MGT (lead), PA (equal)
**Data curation**: AN (lead), PNS (equal), FD (equal)
**Formal analysis**: AN (lead), PNS (equal), FD (equal)
**Funding acquisition**: PA
**Investigation**: MGT (lead), KDT (equal), AN (equal), PNS (equal), FD (equal)
**Methodology**: MGT (lead), KDT (equal), PNS, AD
**Project administration**: PA (lead), KDT (equal)
**Resources:** PA (lead), MGT (equal)
**Supervision:** MGT (lead), PA (equal)
**Validation**: AN (lead), PNS (equal), FD (equal)
**Visualization**: PNS (lead), AN (equal)
**Writing – original draft**: AN (lead), PNS (equal), FD (equal)
**Writing – review & editing**: MGT (lead), AN (equal), PNS

(equal), FD (equal), KDT (equal), PA (equal)

## REFERENCES

[1] S. Aggarwal, A. Qamar, V. Sharma, and A. Sharma, "Abdominal aortic aneurysm: A comprehensive review," *Experimental and Clinical Cardiology*, vol. 16, no. 1, pp. 11–15, 2011.

[2] A. S. Peters, M. Hakimi, P. Erhart, M. Keese, T. Schmitz-Rixen, M. Wortmann, M. S. Bischoff, and D. Böckler, "Current treatment strategies for ruptured abdominal aortic aneurysm," *Langenbeck's archives of surgery*, vol. 401, pp. 289–298, 2016.

[3] G. R. Upchurch Jr, G. A. Escobar, A. Azizzadeh, A. W. Beck, M. F. Conrad, J. S. Matsumura, M. H. Murad, R. J. Perry, M. J. Singh, R. K. Veeraswamy *et al.*, "Society for vascular surgery clinical practice guidelines of thoracic endovascular aortic repair for descending thoracic aortic aneurysms," *Journal of vascular surgery*, vol. 73, no. 1, pp. 55S–83S, 2021.

[4] N. Sakalihasan, J.-B. Michel, A. Katsargyris, H. Kuivaniemi, J.-O. Defraigne, A. Nchimi, J. T. Powell, K. Yoshimura, and R. Hultgren, "Abdominal aortic aneurysms," *Nature Reviews Disease Primers*, vol. 4, no. 1, p. 34, 2018.

[5] E. L. Chaikof, R. L. Dalman, M. K. Eskandari, B. M. Jackson, W. A. Lee, M. A. Mansour, T. M. Mastracci, M. Mell, M. H. Murad, L. L. Nguyen *et al.*, "The society for vascular surgery practice guidelines on the care of patients with an abdominal aortic aneurysm," *Journal of vascular surgery*, vol. 67, no. 1, pp. 2–77, 2018.

[6] K. M. Abdelrahman, M. Y. Chen, A. K. Dey, R. Virmani, A. V. Finn, R. Y. Khamis, A. D. Choi, J. K. Min, M. C. Williams, A. J. Buckler *et al.*, "Coronary computed tomography angiography from clinical uses to emerging technologies: Jacc state-of-the-art review," *Journal of the American College of Cardiology*, vol. 76, no. 10, pp. 1226–1243, 2020.

[7] D. M. Milewicz and F. Ramirez, "Therapies for thoracic aortic aneurysms and acute aortic dissections: old controversies and new opportunities," *Arteriosclerosis, Thrombosis, and Vascular Biology*, vol. 39, no. 2, pp. 126–136, 2019.

[8] J. Anagnostakos and B. K. Lal, "Abdominal aortic aneurysms," *Progress in Cardiovascular Diseases*, vol. 65, pp. 34–43, 2021.

[9] O. Ronneberger, P. Fischer, and T. Brox, "U-net: Convolutional networks for biomedical image segmentation," in *Medical image computing and computer-assisted intervention–MICCAI 2015: 18th international conference, Munich, Germany, October 5-9, 2015, proceedings, part III 18*. Springer, 2015, pp. 234–241.

[10] A. Abdolmanafi, A. Forneris, R. D. Moore, and E. S. Di Martino, "Deep-learning method for fully automatic segmentation of the abdominal aortic aneurysm from computed tomography imaging," *Frontiers in Cardiovascular Medicine*, vol. 9, p. 1040053, 2023.

[11] P. N. Smyrlis, G. R. Stancu, F. Dimaraki, A. Ntetska, T. Karamitsou, K. D. Tzimourta, M. G. Tsipouras, and P. Angelidis, "Aorta localization in computed tomography images: A yolov9 segmentation approach," in *2024 9th South-East Europe Design Automation, Computer Engineering, Computer Networks and Social Media Conference (SEEDA-CECNSM)*, 2024, pp. 163–167.

[12] A. K. Golla, C. Tönnes, T. Russ, D. F. Bauer, M. F. Froelich, S. J. Diehl, S. O. Schoenberg, M. Keese, L. R. Schad, F. G. Zöllner, and J. S. Rink, "Automated screening for abdominal aortic aneurysm in ct scans under clinical conditions using deep learning," *Diagnostics*, vol. 11, no. 11, p. 2131, 2021.

[13] Z. Jiang, H. N. Do, J. Choi, W. Lee, and S. Baek, "A deep learning approach to predict abdominal aortic aneurysm expansion using longitudinal data," *Frontiers in Physics*, vol. 7, p. 235, 2020.

[14] L. Huang, J. Lu, Y. Xiao, X. Zhang, C. Li, G. Yang, X. Jiao, and Z. Wang, "Deep learning techniques for imaging diagnosis and treatment of aortic aneurysm," *Frontiers in Cardiovascular Medicine*, vol. 11, p. 1354517, 2024.

[15] M. Mazonakis and J. Damilakis, "Computed tomography: What and how does it measure?" *European journal of radiology*, vol. 85, no. 8, pp. 1499–1504, 2016.

[16] E. A. Hulten, S. Carbonaro, S. P. Petrillo, J. D. Mitchell, and T. C. Villines, "Prognostic value of cardiac computed tomography angiography: a systematic review and meta-analysis," *Journal of the American College of Cardiology*, vol. 57, no. 10, pp. 1237–1247, 2011.

[17] N. Müller, "Computed tomography and magnetic resonance imaging: past, present and future," *European Respiratory Journal*, vol. 19, no. 35 suppl, pp. 3s–12s, 2002.

[18] D. W. Townsend, J. P. Carney, J. T. Yap, and N. C. Hall, "Pet/ct today and tomorrow," *Journal of Nuclear Medicine*, vol. 45, no. 1 suppl, pp. 4S–14S, 2004.

[19] A. Liberati, D. G. Altman, J. Tetzlaff, C. Mulrow, P. C. Gøtzsche, J. P. A. Ioannidis, M. Clarke, P. J. Devereaux, J. Kleijnen, and D. Moher, "The prisma statement for reporting systematic reviews and meta-analyses of studies that evaluate health care interventions: explanation and elaboration," *Journal of Clinical Epidemiology*, vol. 62, no. 10, pp. e1–e34, Oct 2009, epub 2009 Jul 23.

[20] S. Schueler, G. M. Schuetz, and M. Dewey, "The revised quadas-2 tool," *Annals of internal medicine*, vol. 156, no. 4, p. 323, 2012.

[21] Rayyan Systems Inc., "Rayyan: Accelerating systematic reviews," 2025, accessed: 2025-04-11. [Online]. Available: https://new.rayyan.ai/

[22] A. Ntetska, P. N. Smyrlis, F. Dimaraki, K. Tzimourta, M. G. Tsipouras, and P. Angelidis, "From pixels to prognosis: Deep learning methods in abdominal aortic aneurysm imaging," https://osf.io/7xruy, Nov. 2025, preprint.

[23] C. Mavridis, T. Vagenas, T. Economopoulos, I. Vezakis, O. Petropoulou, I. Kakkos, and G. Matsopoulos, "Automatic segmentation in 3d ct images: A comparative study of deep learning architectures for the automatic segmentation of the abdominal aorta," *Electronics (Switzerland)*, vol. 13, no. 24, 2024.

[24] M. Benčević, M. Habijan, I. Galić, and D. Babin, "Using the polar transform for efficient deep learning-based aorta segmentation in cta images," *2022 International Symposium ELMAR*, pp. 191–194, 2022.

[25] F. Hassan, A. Mahmoud, A. Elnokrashy, and A. Hassan, "Automated deep learning pipeline for accurate segmentation of aortic lumen and branches in abdominal aortic aneurysm: A two-step approach," *2nd International Conference of Intelligent Methods, Systems and Applications, IMSA 2024*, pp. 589–595, 2024.

[26] N. Mu, Z. Lyu, X. Zhang, R. McBane, A. Pandey, and J. Jiang, "Exploring a frequency-domain attention-guided cascade u-net: Towards spatially tunable segmentation of vasculature," *Computers in Biology and Medicine*, vol. 167, 2023.

[27] L. Burrows, K. Chen, W. Guo, M. Hossack, R. McWilliams, and F. Torella, "Evaluation of a hybrid pipeline for automated segmentation of solid lesions based on mathematical algorithms and deep learning," *Scientific Reports*, vol. 12, no. 1, 2022.

[28] D. Chatterjee, T. Shen, P. Mukherjee, S. Lee, J. Garrett, N. Zacharias, P. Pickhardt, and R. Summers, "Automated detection of incidental abdominal aortic aneurysms on computed tomography," *Abdominal Radiology*, vol. 49, no. 2, pp. 642–650, 2024.

[29] Y. Velikova, W. Simson, M. Azampour, P. Paprottka, and N. Navab, "Cactuss: Common anatomical ct-us space for us examinations," *International Journal of Computer Assisted Radiology and Surgery*, vol. 19, no. 5, pp. 861–869, 2024.

[30] A. Saleem Javeed, K. Veeresh, V. Ganesh, C. Lavanya, and B. Parameshachari, "Enhancing segmentation of abdominal aortic aneurysms in ct images," *2023 International Conference on Data Science and Network Security, ICDSNS 2023*, 2023.

[31] M. Habijan, I. Galic, H. Leventic, K. Romic, and D. Babin, "Abdominal aortic aneurysm segmentation from ct images using modified 3d u-net with deep supervision," *Proceedings Elmar - International Symposium Electronics in Marine*, vol. 2020, pp. 123–128, 2020.

[32] A. Abdolmanafi, A. Forneris, R. Moore, and E. Di Martino, "Deep-learning method for fully automatic segmentation of the abdominal aortic aneurysm from computed tomography imaging," *Frontiers in Cardiovascular Medicine*, vol. 9, 2023.

[33] H. Hong and U. Sheikh, "Automatic detection, segmentation and classification of abdominal aortic aneurysm using deep learning," *Proceeding - 2016 IEEE 12th International Colloquium on Signal Processing and its Applications, CSPA 2016*, pp. 242–246, 2016.

[34] S. Koçer, O. Mohamed, and Ö. Dündar, "Disease detection in abdominal ct images using the yolov5 algorithm: A deep learning approach," in *2024 59th International Scientific Conference on Information, Communication and Energy Systems and Technologies (ICEST)*. IEEE, 2024, pp. 1–4.

[35] S. Hahn, C. Morris, D. Bertges, and S. Wshah, "Deep learning for recognition of endoleak after endovascular abdominal aortic aneurysm repair," *Proceedings - International Symposium on Biomedical Imaging*, vol. 2019, pp. 759–763, 2019.

[36] K. Borisova, Y. Fedotova, A. Karpenko, and R. Mullyadzhanov, "Localized growth distribution on the abdominal aortic aneurysm surface using deep learning approaches," *E3S Web of Conferences*, vol. 459, 2023.

[37] F. Brutti, A. Fantazzini, A. Finotello, L. Müller, F. Auricchio, B. Pane, G. Spinella, and M. Conti, "Deep learning to automatically segment and analyze abdominal aortic aneurysm from computed tomography angiography," *Cardiovascular Engineering and Technology*, vol. 13, no. 4, pp. 535–547, 2022.

[38] J.-Q. Zheng, X.-Y. Zhou, C. Riga, and G.-Z. Yang, "Towards 3d path planning from a single 2d fluoroscopic image for robot assisted fenestrated endovascular aortic repair," *Proceedings - IEEE International Conference on Robotics and Automation*, pp. 8747–8753, 2019.

[39] T. Dziubich, P. Białas, Ł. Znaniecki, J. Halman, and J. Brzeziński, "Abdominal aortic aneurysm segmentation from contrast-enhanced computed tomography angiography using deep convolutional networks," *Communications in Computer and Information Science*, vol. 1260, pp. 158–168, 2020.

[40] Y. Wang, M. Zhou, Y. Ding, X. Li, Z. Zhou, Z. Shi, and W. Fu, "Deep learning model for predicting the outcome of endovascular abdominal aortic aneurysm repair," *Indian Journal of Surgery*, vol. 85, pp. 288–296, 2023.

[41] Y. Jung, S. Kim, J. Kim, B. Hwang, S. Lee, E. Kim, J. Kim, and H. Hwang, "Abdominal aortic thrombus segmentation in postoperative computed tomography angiography images using bi-directional convolutional long short-term memory architecture," *Sensors*, vol. 23, no. 1, 2023.

[42] Y. Wang, M. Zhou, Y. Ding, X. Li, Z. Zhou, T. Xie, Z. Shi, and W. Fu, "Fully automatic segmentation of abdominal aortic thrombus in preoperative cta images using deep convolutional neural networks," *Technology and Health Care*, vol. 30, no. 5, pp. 1257–1266, 2022.

[43] K. Lopez-Linares, N. Lete, L. Kabongo, M. Ceresa, G. Maclair, A. Garcia-Familiar, I. Macia, and M. Ballester, "Comparison of regularization techniques for dcnn-based abdominal aortic aneurysm segmentation," *Proceedings - International Symposium on Biomedical Imaging*, vol. 2018, pp. 864–867, 2018.

[44] C. Caradu, A.-L. Pouncey, E. Lakhlifi, C. Brunet, X. Bérard, and E. Ducasse, "Fully automatic volume segmentation using deep learning approaches to assess aneurysmal sac evolution after infrarenal endovascular aortic repair," *Journal of Vascular Surgery*, vol. 76, no. 3, pp. 620–630.e3, 2022.

[45] T. Chung, N. Liang, and D. Vorp, "Artificial intelligence framework to predict wall stress in abdominal aortic aneurysm," *Applications in Engineering Science*, vol. 10, 2022.

[46] T. Dziubich, M. Perdeusz, and A. Skrzynecki, "Assessment of particular abdominal aorta section extraction from contrast-enhanced computed tomography angiography," *International Conference on Human System Interaction, HSI*, vol. 2021, 2021.

[47] T. Zheng, G. Shao, Q. Zhou, Q. Wang, and M. Ye, "Abdominal enhanced computed tomography image by artificial intelligence algorithm in the diagnosis of abdominal aortic aneurysm," *Scientific Programming*, vol. 2021, 2021.

[48] Z. Lyu, N. Mu, M. Rezaeitaleshmahalleh, X. Zhang, R. McBane, and J. Jiang, "Automatic segmentation of intraluminal thrombosis of abdominal aortic aneurysms from ct angiography using a mixed-scale-driven multiview perception network (m2net) model," *Computers in Biology and Medicine*, vol. 179, 2024.

[49] J. R. Camara, R. T. Tomihama, A. Pop, M. P. Shedd, B. S. Dobrowski, C. J. Knox, A. M. Abou-Zamzam Jr, and S. C. Kiang, "Development of a convolutional neural network to detect abdominal aortic aneurysms," *Journal of Vascular Surgery Cases, Innovations and Techniques*, vol. 8, no. 2, pp. 305–311, 2022.

[50] M. Wan, J. Zhu, Y. Che, X. Cao, X. Han, X. Si, W. Wang, C. Shu, M. Luo, and X. Zhang, "Bif-net: Boundary information fusion network for abdominal aortic aneurysm segmentation," *Computers in Biology and Medicine*, vol. 183, 2024.

[51] P. N. Smyrlis, G. R. Stancu, F. Dimaraki, A. Ntetska, T. Karamitsou, K. D. Tzimourta, M. G. Tsipouras, and P. Angelidis, "Aorta localization in computed tomography images: A yolov9 segmentation approach," *2024 9th South-East Europe Design Automation, Computer Engineering, Computer Networks and Social Media Conference (SEEDA-CECNSM)*, pp. 163–167, 2024.

[52] G. Spinella, A. Fantazzini, A. Finotello, E. Vincenzi, G. Boschetti, F. Brutti, M. Magliocco, B. Pane, C. Basso, and M. Conti, "Artificial intelligence application to screen abdominal aortic aneurysm using computed tomography angiography," *Journal of Digital Imaging*, vol. 36, no. 5, pp. 2125–2137, 2023.

[53] Y. Wang, M. Zhou, Y. Ding, X. Li, Z. Zhou, Z. Shi, and W. Fu, "Development and comparison of multimodal models for preoperative prediction of outcomes after endovascular aneurysm repair," *Frontiers in Cardiovascular Medicine*, vol. 9, 2022.

[54] J. Lyu, Y. Fu, M. Yang, Y. Xiong, Q. Duan, C. Duan, X. Wang, X. Xing, D. Zhang, J. Lin, C. Luo, X. Ma, X. Bian, J. Hu, C. Li, J. Huang, W. Zhang, Y. Zhang, S. Su, and X. Lou, "Generative adversarial network-based noncontrast ct angiography for aorta and carotid arteries," *Radiology*, vol. 309, no. 2, 2023.

[55] M. Roby, J. Restrepo, H. Park, S. Muluk, M. K.eskandari, S. Baek, and E. Finol, "Automatic segmentation of abdominal aortic aneurysm from computed tomography angiography using a patch-based dilated unet model," *IEEE Access*, 2025.

[56] Z. Miao, W. Kusakunniran, T. Siriapisith, and P. Saiviroonporn, "Deep learning based technique for classification of abdominal aortic aneurysm (aaa) in ct-scan images," *IEEE Region 10 Annual International Conference, Proceedings/TENCON*, vol. 2022, 2022.

[57] A. Fantazzini, M. Esposito, A. Finotello, F. Auricchio, B. Pane, C. Basso, G. Spinella, and M. Conti, "3d automatic segmentation of aortic computed tomography angiography combining multi-view 2d convolutional neural networks," *Cardiovascular Engineering and Technology*, vol. 11, no. 5, pp. 576–586, 2020.

[58] S. Hahn, M. Perry, C. Morris, S. Wshah, and D. Bertges, "Machine deep learning accurately detects endoleak after endovascular abdominal aortic aneurysm repair," *JVS-Vascular Science*, vol. 1, pp. 5–12, 2020.

[59] L. Zhang, H. Yang, C. Zhou, Y. Li, Z. Long, Q. Li, J. Zhang, and X. Qin, "Artificial intelligence-driven multiomics predictive model for abdominal aortic aneurysm subtypes to identify heterogeneous immune cell infiltration and predict disease progression," *International Immunopharmacology*, vol. 138, 2024.

[60] A. Chandrashekar, A. Handa, P. Lapolla, N. Shivakumar, R. Uberoi, V. Grau, and R. Lee, "A deep learning approach to visualize aortic aneurysm morphology without the use of intravenous contrast agents," *Annals of Surgery*, vol. 277, no. 2, pp. E449–E459, 2023.

[61] A. Salvi, E. Finol, and P. Menon, "3d segmentation of abdominal aortic aneurysm walls from ct angiograms," *Proceedings - 2022 IEEE International Conference on Bioinformatics and Biomedicine, BIBM 2022*, pp. 3873–3875, 2022.

[62] T. Hu, M. Oda, Y. Hayashi, Z. Lu, K. Kumamaru, T. Akashi, S. Aoki, and K. Mori, "Aorta-aware gan for non-contrast to artery contrasted ct translation and its application to abdominal aortic aneurysm detection," *International Journal of Computer Assisted Radiology and Surgery*, vol. 17, no. 1, pp. 97–105, 2022.

[63] S. Kongrat, C. Pintavirooj, and S. Tungjitkusolmun, "Reconstruction of 3d abdominal aorta aneurysm from computed tomographic angiography using 3d u-net deep learning network," *BMEiCON 2022 - 14th Biomedical Engineering International Conference*, 2022.

[64] W. Li, Y. You, S. Zhong, T. Shuai, K. Liao, J. Yu, J. Zhao, Z. Li, and C. Lu, "Image quality assessment of artificial intelligence iterative reconstruction for low dose aortic cta: A feasibility study of 70 kvp and reduced contrast medium volume," *European Journal of Radiology*, vol. 149, p. 110221, 4 2022.

[65] Q. Ma, A. Lucas, H. Hammami, H. Shu, A. Kaladji, and P. Haigron, "Deep-learning approach to automate the segmentation of aorta in non-contrast cts," *Journal of Medical Imaging*, vol. 10, no. 2, 2023.

[66] N. Mu, Z. Lyu, M. Rezaeitaleshmahalleh, X. Zhang, T. Rasmussen, R. McBane, and J. Jiang, "Automatic segmentation of abdominal aortic aneurysms from ct angiography using a context-aware cascaded u-net," *Computers in Biology and Medicine*, vol. 158, 2023.

[67] A. Salvi, E. Finol, and P. G. Menon, "Convolutional neural network based segmentation of abdominal aortic aneurysms," *2021 43rd Annual International Conference of the IEEE Engineering in Medicine & Biology Society (EMBC)*, pp. 2629–2632, 2021.

[68] K. López-Linares, N. Aranjuelo, L. Kabongo, G. Maclair, N. Lete, M. Ceresa, A. García-Familiar, I. Macía, and M. A. González Ballester, "Fully automatic detection and segmentation of abdominal aortic thrombus in post-operative cta images using deep convolutional neural networks," *Medical Image Analysis*, vol. 46, pp. 202–214, 5 2018.

[69] B. Hwang, J. Kim, S. Lee, E. Kim, J. Kim, Y. Jung, and H. Hwang, "Automatic detection and segmentation of thrombi in abdominal aortic aneurysms using a mask region-based convolutional neural network with optimized loss functions," *Sensors*, vol. 22, no. 10, 2022.

[70] S. Mohammadi, M. Mohammadi, V. Dehlaghi, and A. Ahmadi, "Automatic segmentation, detection, and diagnosis of abdominal aortic aneurysm (aaa) using convolutional neural networks and hough circles

algorithm," *Cardiovascular Engineering and Technology*, vol. 10, no. 3, pp. 490–499, 2019.

[71] F. Lareyre, C. Adam, M. Carrier, and J. Raffort, "Automated segmentation of the human abdominal vascular system using a hybrid approach combining expert system and supervised deep learning," *Journal of Clinical Medicine*, vol. 10, no. 15, 2021.

[72] R. Rajmohan, M. Verma, A. Harish, S. S. Raj, S. F. A. S, and R. Divya, "Rupture prediction of abdominal aortic aneursym from ct images using integrated learning models," *2024 International Conference on Electronic Systems and Intelligent Computing (ICESIC)*, pp. 278–283, 2024.

[73] K. López-Linares, L. Kabongo, N. Lete, G. Maclair, M. Ceresa, A. García-Familiar, I. Macía, and M. González Ballester, "Dcnn-based automatic segmentation and quantification of aortic thrombus volume: Influence of the training approach," *Lecture Notes in Computer Science (including subseries Lecture Notes in Artificial Intelligence and Lecture Notes in Bioinformatics)*, vol. 10552, pp. 29–38, 2017.

[74] T. Postiglione, E. Guillo, A. Heraud, A. Rossillon, M. Bartoli, G. Herpe, C. Adam, D. Fabre, R. Ardon, A. Azarine, and S. Haulon, "Multicentric clinical evaluation of a computed tomography-based fully automated deep neural network for aortic maximum diameter and volumetric measurements," *Journal of Vascular Surgery*, vol. 79, no. 6, pp. 1390–1400.e8, 2024.

[75] K. López-Linares, M. Stephens, I. García, I. Macía, M. González Ballester, and R. José Estepar, "Abdominal aortic aneurysm segmentation using convolutional neural networks trained with images generated with a synthetic shape model," *Lecture Notes in Computer Science (including subseries Lecture Notes in Artificial Intelligence and Lecture Notes in Bioinformatics)*, vol. 11794, pp. 167–174, 2019.

[76] R. Epifanov, N. Nikitin, A. Rabtsun, L. Kurdyukov, A. Karpenko, and R. Mullyadzhanov, "Adjusting u-net for the aortic abdominal aneurysm ct segmentation case," *Computer Optics*, vol. 48, no. 3, pp. 418–424, 2024.

[77] C. Adam, D. Fabre, J. Mougin, M. Zins, A. Azarine, R. Ardon, G. d'Assignies, and S. Haulon, "Pre-surgical and post-surgical aortic aneurysm maximum diameter measurement: Full automation by artificial intelligence," *European Journal of Vascular and Endovascular Surgery*, vol. 62, no. 6, pp. 869–877, 2021.

[78] T. Kim, S. On, J. Gwon, and N. Kim, "Computed tomography-based automated measurement of abdominal aortic aneurysm using semantic segmentation with active learning," *Scientific Reports*, vol. 14, no. 1, 2024.

[79] B. Zhang, Z. Lai, S. Liu, X. Xie, X. Zhou, Z. Hou, X. Ma, B. Liu, K. Li, and M. Song, "Sdlu-net: A similarity-based dynamic linking network for the automated segmentation of abdominal aorta aneurysms and branching vessels," *Biomedical Signal Processing and Control*, vol. 100, 2025.

[80] R. Tomihama, J. Camara, and S. Kiang, "Machine learning analysis of confounding variables of a convolutional neural network specific for abdominal aortic aneurysms," *JVS-Vascular Science*, vol. 4, 2023.

[81] T. Siriapisith, W. Kusakunniran, and P. Haddawy, "A retrospective study of 3d deep learning approach incorporating coordinate information to improve the segmentation of pre and post-operative abdominal aortic aneurysm," *PeerJ Computer Science*, vol. 8, 2022.

[82] J.-T. Lu, R. Brooks, S. Hahn, J. Chen, V. Buch, G. Kotecha, K. Andriole, B. Ghoshhajra, J. Pinto, P. Vozila, M. Michalski, and N. Tenenholtz, "Deepaaa: Clinically applicable and generalizable detection of abdominal aortic aneurysm using deep learning," *Lecture Notes in Computer Science (including subseries Lecture Notes in Artificial Intelligence and Lecture Notes in Bioinformatics)*, vol. 11765, pp. 723–731, 2019.

[83] S. Koçer, O. Mohamed, and Ö. Dündar, "Disease detection in abdominal ct images using the yolov5 algorithm: A deep learning approach," *2024 59th International Scientific Conference on Information, Communication and Energy Systems and Technologies (ICEST)*, pp. 1–4, 2024.

[84] B. Zhang, S. Liu, X. Xie, X. Zhou, Z. Hou, M. Song, X. Ma, and L. Zhang, "Towards automated segmentation of human abdominal aorta and its branches using a hybrid feature extraction module with lstm," *Communications in Computer and Information Science*, vol. 1794, pp. 357–368, 2023.

[85] A. Golla, C. Tönnes, T. Russ, D. Bauer, M. Froelich, S. Diehl, S. Schoenberg, M. Keese, L. Schad, F. Zöllner, and J. Rink, "Automated screening for abdominal aortic aneurysm in ct scans under clinical conditions using deep learning," *Diagnostics*, vol. 11, no. 11, 2021.

[86] K. He, X. Zhang, S. Ren, and J. Sun, "Deep residual learning for image recognition," in *Proceedings of the IEEE conference on computer vision and pattern recognition*, 2016, pp. 770–778.

[87] K. Simonyan and A. Zisserman, "Very deep convolutional networks for large-scale image recognition," *arXiv preprint arXiv:1409.1556*, 2014.

[88] A. Krizhevsky, I. Sutskever, and G. E. Hinton, "Imagenet classification with deep convolutional neural networks," *Communications of the ACM*, vol. 60, no. 6, pp. 84–90, 2017.

[89] G. Huang, Z. Liu, L. Van Der Maaten, and K. Q. Weinberger, "Densely connected convolutional networks," in *Proceedings of the IEEE conference on computer vision and pattern recognition*, 2017, pp. 4700–4708.

[90] M. Tan and Q. Le, "Efficientnet: Rethinking model scaling for convolutional neural networks," in *International conference on machine learning*. PMLR, 2019, pp. 6105–6114.

[91] J. Deng, W. Dong, R. Socher, L.-J. Li, K. Li, and L. Fei-Fei, "Imagenet: A large-scale hierarchical image database," in *2009 IEEE conference on computer vision and pattern recognition*. Ieee, 2009, pp. 248–255.

[92] Q. Ma, A. Lucas, A. Kaladji, and P. Haigron, "Deep supervision by gaussian pseudo-label-based morphological attention for abdominal aorta segmentation in non-contrast cts," *Proceedings - International Symposium on Biomedical Imaging*, 2024.

[93] A. Chandrashekar, A. Handa, N. Shivakumar, P. Lapolla, R. Uberoi, V. Grau, and R. Lee, "A deep learning pipeline to automate high-resolution arterial segmentation with or without intravenous contrast," *Annals of Surgery*, vol. 276, no. 6, pp. E1017–E1027, 2022.

[94] K. López-Linares, N. Aranjuelo, L. Kabongo, G. Maclair, N. Lete, M. Ceresa, A. García-Familiar, I. Macía, and M. González Ballester, "Fully automatic detection and segmentation of abdominal aortic thrombus in post-operative cta images using deep convolutional neural networks," *Medical Image Analysis*, vol. 46, pp. 202–214, 2018.

[95] G. van Praagh, P. Nienhuis, M. Reijrink, M. Davidse, L. Duff, B. Spottiswoode, D. Mulder, N. Prakken, A. Scarsbrook, A. Morgan, C. Tsoumpas, J. Wolterink, K. Mouridsen, R. Borra, B. Sinha, and R. Slart, "Automated multiclass segmentation, quantification, and visualization of the diseased aorta on hybrid pet/ct–sequoia," *Medical Physics*, vol. 51, no. 6, pp. 4297–4310, 2024.

[96] D. Ginzburg, S. Nowak, U. Attenberger, J. Luetkens, A. Sprinkart, and D. Kuetting, "Computer tomography-based assessment of perivascular adipose tissue in patients with abdominal aortic aneurysms," *Scientific Reports*, vol. 14, no. 1, 2024.

[97] N. Mu, Z. Lyu, X. Zhang, R. McBane, A. S. Pandey, and J. Jiang, "Exploring a frequency-domain attention-guided cascade u-net: Towards spatially tunable segmentation of vasculature," *Computers in biology and medicine*, vol. 167, p. 107648, 2023.

[98] J. Raffort, C. Adam, M. Carrier, A. Ballaith, R. Coscas, E. Jean-Baptiste, R. Hassen-Khodja, N. Chakfé, and F. Lareyre, "Artificial intelligence in abdominal aortic aneurysm," *Journal of vascular surgery*, vol. 72, no. 1, pp. 321–333, 2020.

[99] S. Baek and A. Arzani, "Current state-of-the-art and utilities of machine learning for detection, monitoring, growth prediction, rupture risk assessment, and post-surgical management of abdominal aortic aneurysms," *Applications in Engineering Science*, vol. 10, p. 100097, 2022.

[100] M. R. Kodenko, Y. A. Vasilev, A. V. Vladzymyrskyy, O. V. Omelyanskaya, D. V. Leonov, I. A. Blokhin, V. P. Novik, N. S. Kulberg, A. V. Samorodov, O. A. Mokienko *et al.*, "Diagnostic accuracy of ai for opportunistic screening of abdominal aortic aneurysm in ct: A systematic review and narrative synthesis," *Diagnostics*, vol. 12, no. 12, p. 3197, 2022.

[101] T.-W. Wang, Y.-H. Tzeng, J.-S. Hong, H.-R. Liu, K.-T. Wu, H.-N. Fu, Y.-T. Lee, W.-H. Yin, and Y.-T. Wu, "Deep learning models for aorta segmentation in computed tomography images: A systematic review and meta-analysis," *Journal of Medical and Biological Engineering*, vol. 44, no. 4, pp. 489–498, 2024.

[102] T.-W. Wang, Y.-H. Tzeng, J.-S. Hong, H.-R. Liu, H.-N. Fu, Y.-T. Lee, W.-H. Yin, and Y.-T. Wu, "The role of deep learning in aortic aneurysm segmentation and detection from ct scans: A systematic review and meta-analysis," *Next Research*, p. 100059, 2024.

[103] J. Sokol and P. K. Nguyen, "Risk prediction for abdominal aortic aneurysm: One size does not necessarily fit all," *Journal of Nuclear Cardiology*, vol. 30, no. 2, pp. 814–817, 2023.

[104] V. Larivière, D. Pontille, and C. R. Sugimoto, "Investigating the division of scientific labor using the contributor roles taxonomy (credit)," *Quantitative science studies*, vol. 2, no. 1, pp. 111–128, 2021.

**AIMILIA NTETSKA** is currently a Ph.D. Candidate with the Department of Electrical and Computer Engineering, University of Western Macedonia, Greece. She received her diploma in Electrical and Computer Engineering from the same department, specializing in Electronics and Computer Science. Her diploma thesis focused on the analysis of electroencephalogram (EEG) data using brain–computer interface technology. Her research interests include EEG signal analysis, brain–computer interfaces, and the application of artificial intelligence to neurological disorder diagnosis and assessment. She has participated in several research projects, including IntelliWheelChair, Agrotour, Deep in Biopsies and safeAorta, aimed at developing AI-driven healthcare solutions. She has also co-authored 5 publication including peer reviewed conference papers in proceedings and journal articles.

**PANAGIOTIS N. SMYRLIS** is a PhD student in the department of Electrical and Computer Engineering in the University of Western Macedonia, Kozani, Greece, and received his MEng degree from the Informatics and Telecommunications Engineering Department (now Elecrical and Computer Engineering department). His research focuses on Machine and Deep Learning theory and applications. He has co-authored 12 research papers, seen in peer-reviewed conference proceedings and scientific journals in literature. His research interests include biomedical engineering, novel Machine/Deep Learning methods and their application on different data scenarios for Decision Support. He has been an associate / patner on various research projects during the last decay. Moreover, he has been a teaching assistant in the university of Western Macedonia on Signal Processing, Numerical Analysis, Data Mining and Computer programming related courses.

**FOTEINI DIMARAKI** is a graduate of the Department of Informatics and Telecommunications Engineering of the Polytechnic School of the University of Western Macedonia (2022) and a PhD Candidate from April 2022 in the same department. Her main research interests include machine learning and algorithm analysis in the field of Agriculture and Smart Farming. She has published 4 papers in scientific journals and conferences on this subject.

**KATERINA D. TZIMOURTA** is Postdoctoral Researcher in the Dept. of Electrical and Computer Engineering, Univ. of Western Macedonia and an Adjunct Lecturer in the Dept. of Informatics and Telecommunications, Univ. of Ioannina, Greece. She is an IT Engineer by education and she focuses on the analysis of electroencephalographic (EEG) signals acquired from clinical EEG recordings and data acquired from wearable devices for brain and cognitive disorders' analysis. Over the past 3 years she has developed a diverse set of skills, encompassing teaching abilities, research expertise, and administrative competencies.

**MARKOS G. TSIPOURAS** Markos G. Tsipouras is a Prof. on Signal Processing in the Department of Electrical and Computer Engineering in the University of Western Macedonia, Kozani, Greece. He received the diploma degree in Computer Science from the University of Ioannina, Greece, in 1999, and M.Sc. and Ph.D degrees in computer science, in 2002 and 2008 respectively, from the same department. Also, he received a Natural Sciences diploma from the Hellenic Open University in 2013. He has been appointed Honorary Senior Research Fellow in the Department of Metabolism, Digestion and Reproduction, atvImperial College of London. He has published more than 200 papers in peer-reviewedv scientific journals, conference proceedings and book chapters. Also, he has been involved in in more than 30 European (3rd CSF, FP6, FP7, H2020) and National Research Projects. His research interests include biomedical signal and image processing, medical informatics, artificial intelligence and data mining.

**PANTELIS ANGELIDIS** is a Prof. on Bioinformatics and Digital Health in the Department of Electrical and Computer Engineering in the University of Western Macedonia, Kozani, Greece since 2008. He is a Telecommunication and Computer Engineer by education. He has worked on Technology for Health projects in Europe, US and Africa for the past 30 years. He has published over 130 papers in international journals, conferences and book chapters. He is the founder of Vidavo (http://www.vidavo.eu/), a Digital Health start-up. He has patented three telemedicine devices and one data processing algorithm. He was visiting professor at MIT Media Lab in 2009-10 and again in 2015-16, at UB Medical School, Barcelona and Kingston Un, UK. He is a visiting Prof. at DIKU/UCPH, Copenhagen. He is a Marshall Memorial fellow and an alumni of the Bodosaki foundation. He is a Member of the Hellenic Innovation Network. He is active in turning research results into innovative products focusing on technologies for preventive health, personalized medicine and active ageing.